ADVANCED OPTICAL MATERIALS
www.advopticalmat.de

Wavelength-Tunable Micro/Nanolasers

Ming-Hua Zhuge, Caofeng Pan, Yazhi Zheng, Jianbin Tang, Salman Ullah, Yaoguang Ma, and Qing Yang**

Micro/nanolasers (MNLs) emit coherent light on the micro/nanoscale. Research on the application of MNLs has progressed rapidly in the past two decades because of their great potential for optoelectronics with compact sizes, low cost, and low energy consumption. Wavelength-tunable MNLs are essential for a variety of fields including optical communications, solid-state lighting, and on-chip wavelength-division multiplexing. Thus far, tremendous progress is achieved toward the development of wavelength-tunable MNLs based on bandgap tuning and cavity design. Lasing wavelength is substantially defined by material bandgap, tuned by changing the geometry of the cavity structures, and can also, to some extent, be influenced by operational environment. This review is focused on the intrinsic merits of wavelength-tunable MNLs, and the recent progress is examined. Bandgap engineering, materials synthesis, cavity structure design, wavelength-tuning principles, and lasing performance are explored and systematically discussed. Finally, the current research status and perspectives on possible future applications are summarized.

1. Introduction

Since Theodore Maiman first demonstrated lasing experimentally in ruby in 1960,[1] lasers have become an indispensable technology promoting industrial development, revolutionizing data communication techniques, and driving fundamental research in almost every scientific field. The advantageous features of small lasers include ultrafast dynamics,[2] high compactness,[3] and high emitting efficiencies.[4] Owing to these advantages, decreasing the physical size of a laser system has been one of the prevalent themes since the birth of lasers. Since 1992, the field of MNLs has witnessed the introduction of pioneering technologies (**Figure 1**) like microdisk lasers,[5–7] photonic crystal lasers,[8–10] and nanowire lasers,[11–13] metallic-coated nanolasers,[14–20] plasmonic nanowire lasers,[21–34] etc.

Thus far, MNLs have demonstrated a vast potential for applications in a wide variety of areas such as optical communications, high-density data storage, sensors, and biocompatible detectors.[35–41] The optimization of their parameters, including wavelength, mode, threshold, polarization, etc., is of great significance in the pursuing of practical applications.[42] Compared with wavelength-fixed MNLs, multiwavelength[43,44] and wavelength-tunable MNLs capable of emitting coherent light within a wide spectral range represent particularly interesting opportunities for on-chip optoelectronics,[45] optical integration,[46] as well as super-resolution imaging.[47] Over the past decade, tremendous progress has been achieved in the development of wavelength-tunable MNLs based on bandgap tuning and cavity design (**Figure 2**).

Remarkable advancements have been made regarding bandgap engineering based on alloying semiconductor nanomaterials, especially using II–VI and III–V semiconductors and their alloys,[48–55] organic and inorganic halide perovskites,[56–63] and emerging 2D transition metal dichalcogenides (TMDCs) materials.[64–72] Bandgap is a critical parameter of semiconductor materials, which is largely defined by the material structure. Alloying several individual semiconductors allows for the synthesis of different materials with a wide range of bandgaps. At present, an incredible variety of alloying materials have been exhibited by researchers in the field. Research works on II–VI and III–V mesoscopic semiconductor materials, including $Zn_xCd_{1-x}S$,[73] $In_xGa_{1-x}N$,[74] CdS_xSe_{1-x},[75] $Zn_xCd_{1-x}S_ySe_{1-y}$,[76] $GaAs_yP_{1-y}$,[77] $Al_xGa_{1-x}P$,[77] $Al_xGa_{1-x}N$,[78] $Cd_xPb_{1-x}S$,[79] $GaAs_{1-x}Sb_x$,[80] and $In_xGa_{1-x}P$,[81] have been a boost in recent years. For perovskites, $MAPbX_3$ ($MA^+ = CH_3NH_2^+$, methylammonium; $X^- = I^-$, Br^-, Cl^-),[82] $FAPbX_3$ ($FA^+ = CH(NH_2)_2^+$,

M.-H. Zhuge, Y. Zheng, S. Ullah, Prof. Y. Ma, Prof. Q. Yang
State Key Laboratory of Modern Optical Instrumentation
College of Optical Science and Engineering
Zhejiang University
Hangzhou 310027, China
E-mail: mayaoguang@zju.edu.cn; qingyang@zju.edu.cn
Prof. C. Pan
Beijing Institute of Nanoenergy and Nanosystems
Chinese Academy of Sciences
National Center for Nanoscience and Technology
Beijing 100083, China
Prof. J. Tang
Key Laboratory of Biomass Chemical Engineering
of Ministry of Education
Center for Bionanoengineering
Department of Chemical and Biological Engineering
Zhejiang University
Hangzhou 310027, China
Prof. Q. Yang
Collaborative Innovation Center of Extreme Optics
Shanxi University
Taiyuan 030006, China
The ORCID identification number(s) for the author(s) of this article can be found under https://doi.org/10.1002/adom.201900275.

DOI: 10.1002/adom.201900275

© 2019 WILEY-VCH Verlag GmbH & Co. KGaA, Weinheim

formamidinium),[83] $CsPbX_3$,[84] $CsSnX_3$,[85] and $CsPbMBr_3$ (M^{2+} = Sn^{2+}, Cd^{2+}, Zn^{2+})[86] have been demonstrated experimentally and provided a huge family of gain media choices. Meanwhile, numerous progress has been achieved in the development of a broad range of notable 2D TMDCs materials, including $MoS_{2(1-x)}Se_{2x}$,[87,88] $Mo_{1-x}W_xSe_2$,[89] $WS_{2(1-x)}Se_{2x}$,[90] $SnSe_{2(1-x)}S_{2x}$,[91] $Mo_{1-x}W_xS_2$,[92] $Co_{1-x}W_xS_2$,[93] $WSe_{2(1-x)}Te_{2x}$,[94] and $Mo_{1-x}W_xTe_2$.[95] One important feature shared by these composition-varied micro/nanomaterials is the controllable bandgaps, which span the visible spectrum and extend into both the UV and IR ranges.

Cavity design is another effective strategy for achieving tunable lasing wavelengths (**Table 1**). In this approach, changing the geometry of the cavity structure[96–99] or the refractive index[100] of the cavity results in changes in the resonance modes and free spectral range, which can be utilized to select specific lasing wavelengths. The importance of cavity design lies in two factors: (1) A MNL with a particular structure can be made tunable by changing the resonators;[101] (2) The variable wavelength only lases when the newly designed cavity satisfies the threshold condition.[102–105]

In order to satisfy the threshold conditions under a range of lasing wavelengths, cavity design is also usually companioned with bandgap tuning, Burstein–Moss effect,[106] or intrinsic self-absorption.[107–109] Furthermore, as shown in Figure 2, lasing wavelength can also be tuned to some extent via environmental conditions, such as temperature,[110] pressure,[111] and strain.[112–114]

In this review, we present the recent progress in the field of wavelength-tuning MNLs. In Section 2, we consider wavelength-tunable MNLs based on bandgap tuning, paying particular attention to the composition-varied materials such as II–VI and III–V semiconductors, halide perovskites, and 2D TMDCs materials. In Section 3, we discuss the cavity design approach enabled wavelength-tunable MNLs. Then, in Section 4, we focus on the advances of tunable emission wavelengths via the combination of bandgap tuning and cavity design. Section 5 exhibits the lasing wavelength tunability induced by environmental conditions. Finally, we conclude in Section 6 with a summary of the practical applications and current progress in the field and highlight the scientific and engineering challenges driving the development of next-generation wavelength-tunable MNLs.

Minghua Zhuge is a Ph.D. student in College of Optical Science and Engineering at Zhejiang University, China, under the supervision of Qing Yang. She is interested in nanophotonics, micro/nanomaterials, micro/nanolasers, and the parameter optimization, and their practical applications such as spectroscopy and biocompatible probes.

Yaoguang Ma received his Ph.D. degree from Zhejiang University, China, in 2012. After that, he worked as postdoc researcher at Peking University, University of California, San Diego, CA, and University of Colorado Boulder, USA. Currently, he is a tenure-track professor in College of Optical Science and Engineering at Zhejiang University. His research interests are in the fundamentals of nanoscale light–matter interactions and the converged applications of nanotechnologies in modern optical systems.

Qing Yang received her Ph.D. degree from College of Materials Science and Engineering at Zhejiang University, China, in 2006. She worked as a visiting scientist in Department of Material Science and Engineering at Georgia Institute of Technology, USA, from 2009 to 2012. Currently, she is a professor in College of Optical Science and Engineering at Zhejiang University. Her research group focuses on micro/nanophotonics, nanomaterials, and spatial super-resolution imaging.

2. Bandgap Tuning for Wavelength-Tunable MNLs

2.1. Traditional II–VI and III–V Semiconductors

Semiconductor micro/nanomaterials such as nanowires and microrods[12,115,116] have single-crystalline structures, excellent geometric uniformities, subwavelength transverse dimensions, and relatively high refractive indices, making them ideal candidate for MNLs. The growth of complex semiconductor nanostructured alloys on Si substrates[117,118] presents an excellent opportunity for controlling the spatially varied composition and produce a wide range of bandgaps within a single substrate in a single synthesis run.[119] Several chemical vapor deposition methods have been applied to this end.[120] One method is the utilization of two kinds of source materials separated at two different axial locations. By employing a temperature gradient along the axial direction, moving the sources changes their sublimation temperature and therefore determines the relative amount of the two gas-phase source materials on the substrate. This source material gradient method (**Figure 3**a), first demonstrated by Kuykendall et al. for the growth of an InGaN alloy,[74] offers a range of possible In/Ga ratios. The photoluminescence (PL) of the as-synthesized nanowires covers the wavelength

© 2019 WILEY-VCH Verlag GmbH & Co. KGaA, Weinheim

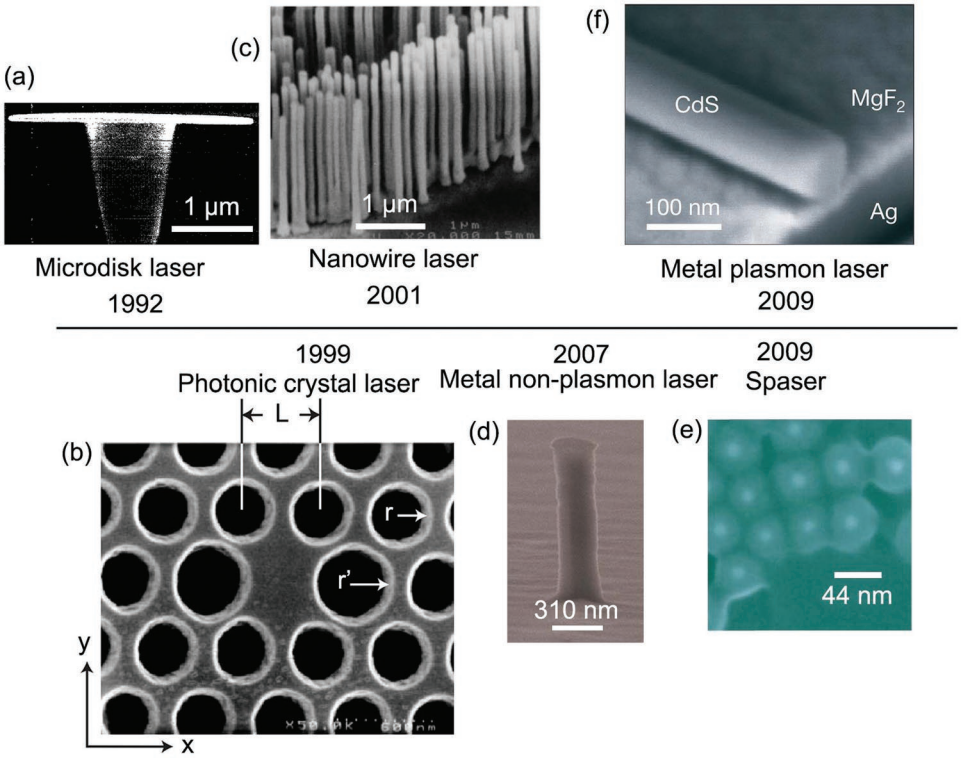

Figure 1. Development timeline of MNLs. a) Microdisk laser. Reproduced with permission.[5] Copyright 1992, American Institute of Physics. b) Photonic crystal laser. The interhole spacing (L) is 515 nm, and the radius of the holes (r) is ≈180 nm. The two enlarged holes have a radius (r') of 240 nm. Reproduced with permission.[8] Copyright 1999, American Association for the Advancement of Science. c) Nanowire laser. Reproduced with permission.[11] Copyright 2001, American Chemical Society. d) Metal nonplasmon laser. Reproduced with permission.[129] Copyright 2007, Springer Nature. e) Spaser. Reproduced with permission.[131] Copyright 2009, Springer Nature. f) Metal plasmon laser. Reproduced with permission.[132] Copyright 2009, Springer Nature.

from 325 to 850 nm (Figure 3c,d), allowing complete composition tunability from pure GaN to InN with no composition miscibility gap in the nanowire form.

A complementary approach called temperature gradient method depends on alloy compositions on the nonuniform temperature of the substrate.[51,73,75] This approach allows the two source materials to be placed in the same tube, while the substrate is placed horizontally along the tube direction in the downstream of the gas flow. It is particularly important that the growth temperature profile is optimized for the growth of varied compositions. A substrate with spatially composition-varied nanowire lasers could emit coherent light covering the entire emission spectrum has been successfully demonstrated by controlling the local substrate temperature of the chemical vapor deposition (CVD) system in a single growth run (Figure 3e).[75]

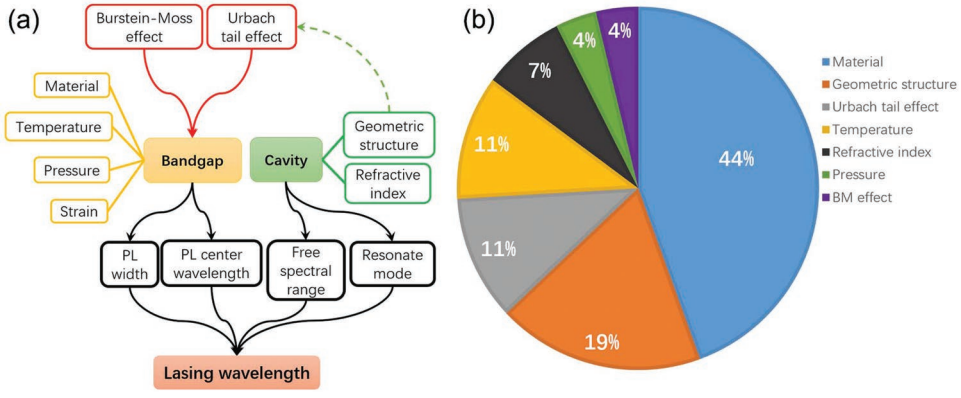

Figure 2. Elements influence lasing wavelength. a) The graph shows the relationship between different elements and lasing wavelength. b) Elements take different portions in the overall reported results, which show that 44% wavelength-tuning MNLs are demonstrated to be realized based on composition-varied materials.

© 2019 WILEY-VCH Verlag GmbH & Co. KGaA, Weinheim

Table 1. Brief history of wavelength-tunable MNLs: strategies, principles, features, and performances.

Year	Gain medium	Variable	Size	Lasing wavelength [nm]	Range [nm]	Threshold	Temperature	Ref.
2005	Multi-ZnCdS NB	Composition	Thickness: ≈60 nm; Width: ≈3 μm; Length: ≈300 μm	373, 393, 513		≈100 kW cm^{-2}	RT	[73]
2006	Single GaN NW	Cavity	Length: ≈24 μm	≈370–380	<10	≈75 μJ cm^{-2}	RT	[189]
2008	Multi-InGaN MQW NW	Composition	Width: ≈500 nm; Length: 50 μm	365–494	129	≈900 kW cm^{-2}	RT	[128]
2009	CdSSe array	Composition	0.3 cm × 1.2 cm	≈500–700	≈200	≈300 kW cm^{-2}	77 K	[75]
2009	Single CdSe, CdS, ZnO NWs	Composition	Length: ≈1 mm; Diameter: 3.3 μm	743, 519, 391		≈1 μJ	RT	[43]
2011	Single CdSe NW	Cavity	Diameter: 240 nm; Length: 84 μm	733.7–726.9	6.8	50 μJ cm^{-2}	RT	[191]
2012	Single CdS NB	Cavity	≈5 μm × 4 μm	490–502	12	≈4 GW cm^{-2}	RT	[197]
2013	Single CdSe NW	Urbach tail effect and cavity	Diameter: 402 nm; Length: 289–288 μm	746–706	40	≈50 μJ cm^{-2}	RT	[108]
2013	Multi-CdS NW	Urbach tail effect and cavity	Diameter: ≈250 nm; Length: 4.3–16.4 μm	495–516	21	≈5 μJ cm^{-2}	RT	[198]
2013	Single CdSSe NW	Composition and cavity	Length: 200 μm;	530, 637		≈8 kW cm^{-2}	RT	[127]
2013	Single CdSSe NB	Composition and cavity	Length: 127 μm; Diameter: 3 μm	578, 598, 621, 640		≈50 MW cm^{-2}	RT	[124]
2013	Multi-CdS NW	BM effect and cavity	Diameter: ≈220 nm; Length: ≈10 μm	504–483	21	≈2 μJ cm^{-2}	RT	[204]
2013	Single GaAs/AlGaAs NW	Temperature	Diameter: 340 nm; Length: 11.4 μm	827–892	65	≈2.4 kW cm^{-2}	10–285 K	[205]
2014	Single CdSSe NW	Composition and cavity	Diameter: ≈450 nm; Length: ≈435–438 μm	636–517	119	≈20 kW cm^{-2}	RT	[102]
2014	Multi-InGaN NR	Composition	Diameter: ≈50 nm; Length: ≈200 nm	474–627	53	≈100 W cm^{-2}	7 K	[25]
2015	Multi-$MAPbX_3$ NW	Composition	Length: ≈20 μm	787–490	≈287	≈500 nJ cm^{-2}	RT	[151]
2015	IR 140	Cavity: Substrate *n*	NP array area: ≈1 cm^2	853–896	43	0.188 mJ cm^{-2}	RT	[100]
2015	IR 140	Cavity: Liquid *n*	NP array area: ≈1 cm^2	862–891	29	0.188 mJ cm^{-2}	RT	[100]
2015	Single GaN NW	Pressure	Diameter: ≈140 nm Length: ≈5 μm	≈335–365	≈30	≈1.5 MW cm^{-2}	RT	[126]
2015	Single $MAPbI_3$ NW	Temperature	Length: ≈10 μm Diameter: ≈200 nm	≈780–795 ≈745–755	≈15 ≈10	≈11 μJ cm^{-2}	300–160 K 140–80 K	[206]
2016	Multi-$(MA,FA)PbX_3$ NW	Composition	Length: ≈20 μm Width: ≈300 nm	≈824–490	≈334	≈10 μJ cm^{-2}	RT	[171]
2016	Single ZnO NW	Temperature	Diameter: 70 nm Length: 1.7 μm	372–386	14	≈50 MW cm^{-2}	77–353 K	[28]
2016	Multi-$CsPbX_3$ NW	Composition	Length: ≈50 μm Width: ≈200 nm	≈420–710	≈290	≈30 μJ cm^{-2}	RT	[163]
2017	Multi-$CsPbX_3$ M/NR	Composition	Length: ≈10 μm Diameter: ≈1 μm	428–668	240	≈14.1 μJ cm^{-2}	RT	[158]
2017	Single InGaN MR	Composition and cavity	Diameter: ≈2 μm Length: 10 μm	372–408	36	≈100 kW cm^{-2}	RT	[201]
2017	Multi-CdS NW	Urbach tail effect and cavity	Diameter: ≈130 nm Length: 5.2–26.4 μm	465–491	26	≈75 μJ cm^{-2}	77 K	[193]
2018	IR 140	Cavity	4 mm × 4 mm	≈860–880	20	≈0.3 mJ cm^{-2}	RT	[105]
2018	Single ZnO MW	Gain medium *n*	Diameter: ≈5 μm Length: ≈1 mm	≈390–400	<10	≈15.1 mW	RT	[213]

Note: NB, nanobelt; NW, nanowire; NR, nanorod; MA^+, $CH_3NH_2^+$, methylammonium; FA^+, $CH(NH_2)_2^+$, formamidinium; X, (I, Br, Cl); MR, microrod; MW, microwire; MQW, multiquantum well; BM, Burstein–Moss; *n*, refractive index; NP, nanoparticle; RT, room temperature.

© 2019 WILEY-VCH Verlag GmbH & Co. KGaA, Weinheim

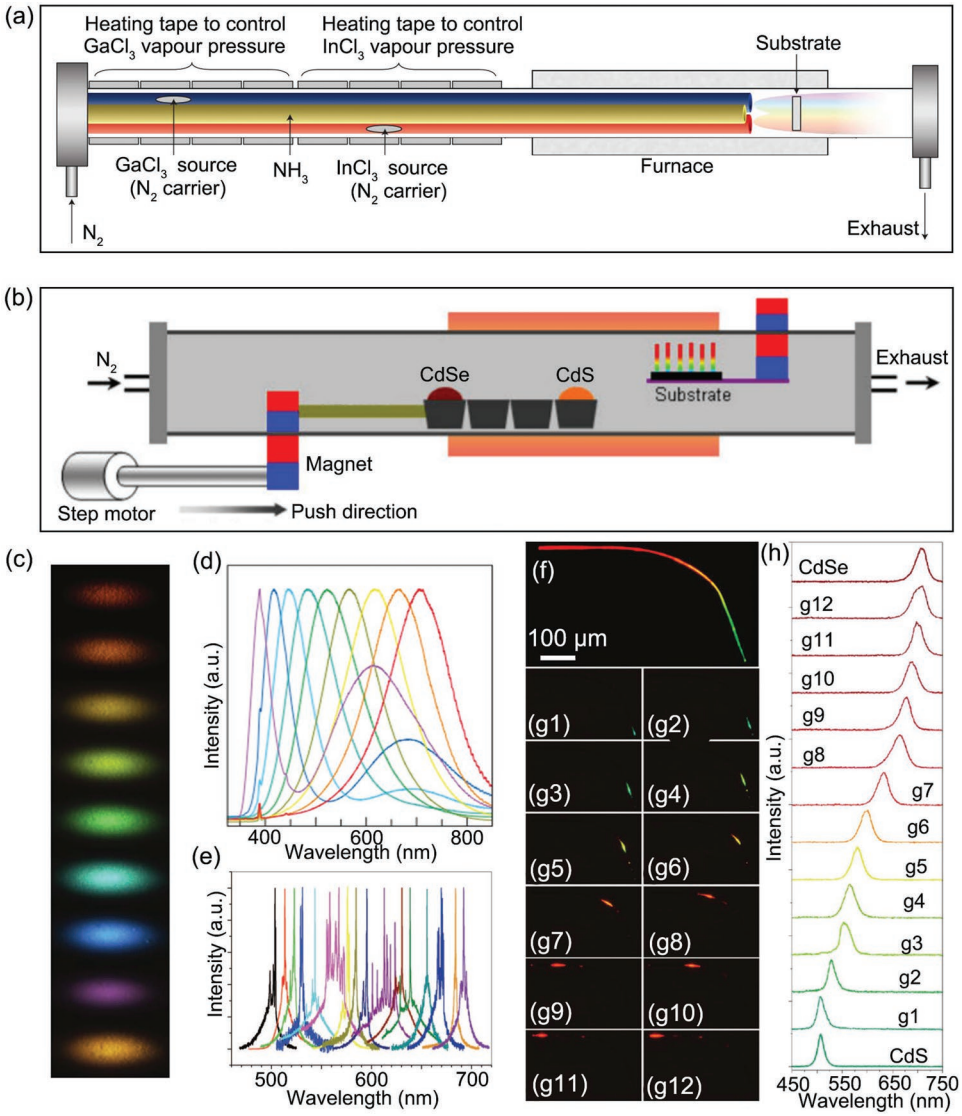

Figure 3. Spatial composition grading synthesis engineering. a) Experimental setup of the source material gradient method. Two independently controlled heating tapes were used to tune the vapor pressure of the $InCl_3$ and $GaCl_3$ precursors. Reproduced with permission.[74] Copyright 2007, Springer Nature. b) Experimental setup for growing multicolor CdSSe NWs. Reproduced with permission.[121] Copyright 2011, American Chemical Society. c) Color charge-coupled device (CCD) images show the emission at different position from the $In_xGa_{1-x}N$ nanowire arrays and d) visible PL emission (x = 0–0.6) demonstrates that the peaks shift to longer wavelengths with increasing x. Reproduced with permission.[74] Copyright 2007, Springer Nature. e) Different PL collected at various locations along the substrate maintained at 77 K under optical pump showing lasing or multimode lasing. Reproduced with permission.[75] Copyright 2009, American Chemical Society. f) Color CCD images of a representative CdSSe NW illuminated under optical pump; g1–12) color CCD images of different spots along the length, pumped locally with a beam of focused 405 nm laser; h) the corresponding local PL spectra collected from these excited spots in g1–12, respectively. Reproduced with permission.[121] Copyright 2011, American Chemical Society.

The excellent benefits aside, these two methods each has obvious deficiencies—which hints toward the possibility of combining them to conquer their respective inherent defects. Gu et al. proposed a facile source-moving thermal evaporation method for composition-graded CdSSe nanowire growth in a horizontal quartz tube mounted inside a single-zone furnace (Figure 3b).[121] One alumina boat containing CdS powder is fixed in the center of the heating zone. Another alumina boat containing CdSe powder, which is first placed in the upstream of the tube and outside the heating zone, is then moved by a step motor along the tube during growth. The source-moving thermal evaporation method has proven to be highly flexible.[76,122,123] This approach has successfully enhanced the control of alloy composition and bandgap with a single substrate and a single growth run to the realization of gradual composition and bandgap variation in a single nanostructure (Figure 3f). The center wavelength of the PL spectra along the length of NWs is continuously and gradually changed from 505 nm at the green end to 710 nm at the red end (Figure 3g,h).

Complete compositional variation in single nanostructures is a critical step in the process of attaining wide-range wavelength tunability. These innovative chemical growth techniques

© 2019 WILEY-VCH Verlag GmbH & Co. KGaA, Weinheim

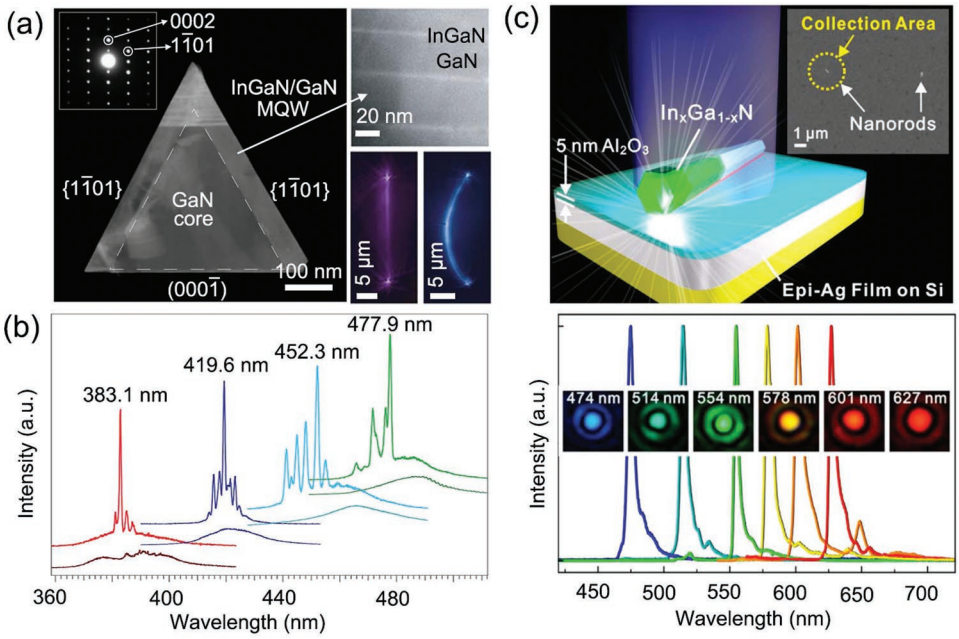

Figure 4. Lasing wavelength-tunable devices based on multiple semiconductor micro/nanostructures. a) Dark-field cross-sectional STEM image recorded of a 26MQW nanowire structure. Upper right: Dark-field cross-sectional STEM image of 3MQW. Upper left inside: Corresponding electron diffraction pattern. Lower right: PL images (false color) recorded from GaN/$In_{0.05}Ga_{0.95}N$ (left) and GaN/$In_{0.23}Ga_{0.77}N$ (right) MQW nanowire structures. b) Normalized PL spectra collected from four representative 26MQW nanowire structures with increasing In composition pumped at ≈250 and ≈700 kW cm^{-2}, respectively. (a,b) Reproduced with permission.[128] Copyright 2008, Springer Nature. c) Schematic diagram of the nanolaser structure: Single $In_xGa_{1-x}N$@GaN core–shell nanorods were dispersed on the Al_2O_3-covered epitaxial Ag film. Upper right: the SEM image of a single nanorod. The lower: all-color, single-mode lasing images and spectra observed from single nanorods with an emission line width ≈4 nm. Reproduced with permission.[25] Copyright 2014, American Chemical Society.

have boosted the development of white-light emission,[122,123] multiwavelength MNLs,[44,124,125] and wavelength-tunable MNLs.[102,126,127]

As shown in **Figure 4**a,b, InGaN multi-quantum-wells (MQW) nanowire heterostructures have yielded lasing with composition-dependent emission from 365 to 494 nm.[128] Through exploring the growth time, temperature, and repeat periods during MQW deposition, ratio of In composition as well as the InGaN/GaN quantum-well unit thickness and numbers can all be precisely controlled. The variation of In composition has led to lasing wavelength tuning.

Lasers based on dielectric resonators are intrinsically limited in their size because of the diffraction limit of light. Bergman and Stockman proposed concept of surface plasmon amplification by stimulated emission of radiation, or spaser[129–131] could break this limit where an amplifier comprising localized surface plasmons oscillates at metal–dielectric interfaces. Recently, this concept has gained an increasing interest due to the ability of a plasmon-based oscillator[132] to confine resonant light on a scale approaching or breaking the diffraction limit.[133] Recently, another effective approach was reported comprising gain-composition-tunable semiconductor nanomaterials with surface plasmon polaritons (SPP). In this method,[25] the emission wavelength depends on the proportion of In composition in the gain medium and can be tuned from near-infrared (InN, 0.65 eV) to near-ultraviolet (GaN, 3.4 eV). Benefiting from a large reported gain coefficient of 10^4 cm^{-1}, InGaN is one of the most appropriate optical material to compensate the intrinsic Ohmic loss of plasmon lasers. The $In_xGa_{1-x}N$/GaN core–shell nanorods with different x-values were dispersed on an Al_2O_3-covered epitaxial Ag film exhibiting lasing wavelength from 474 to 627 nm (Figure 4c). For vertical-cavity surface-emitting lasers and other conventional lasers, the resonator length must be changed to spatially and spectrally match the particular emission wavelength generated from the gain medium. In comparison, the all-color plasmonic nanorod laser is not restricted by this constraint. Combined with the novel autotuning mechanism resulting from the interplay between the gain media and the plasmonic cavity material (Ag), a single-mode wavelength-tunable MNL is achieved.

2.2. Organic–Inorganic Halide Perovskite Alloy Nanostructures

Organic–inorganic or metal halide perovskites, with the general formula ABX_3 (where A is a cation larger than B), represent a large family of interesting compounds[134] where X can be carbides, nitrides, halides, and hydrides. The organic–inorganic hybrid perovskites have strong optical absorption, promising optical gain, low trap state densities, long charge carrier lifetime, and long exciton diffusion lengths. These physical properties are advantageous especially for application in efficient photovoltaics,[135,136] light-emitting diodes,[137–142] photodetectors,[143–145] and other thin-film optoelectronic devices.[146,147]

The past five years have seen a renaissance of halide perovskites ABX_3 (where A is an organic ammonium cation or Cs^+,

© 2019 WILEY-VCH Verlag GmbH & Co. KGaA, Weinheim

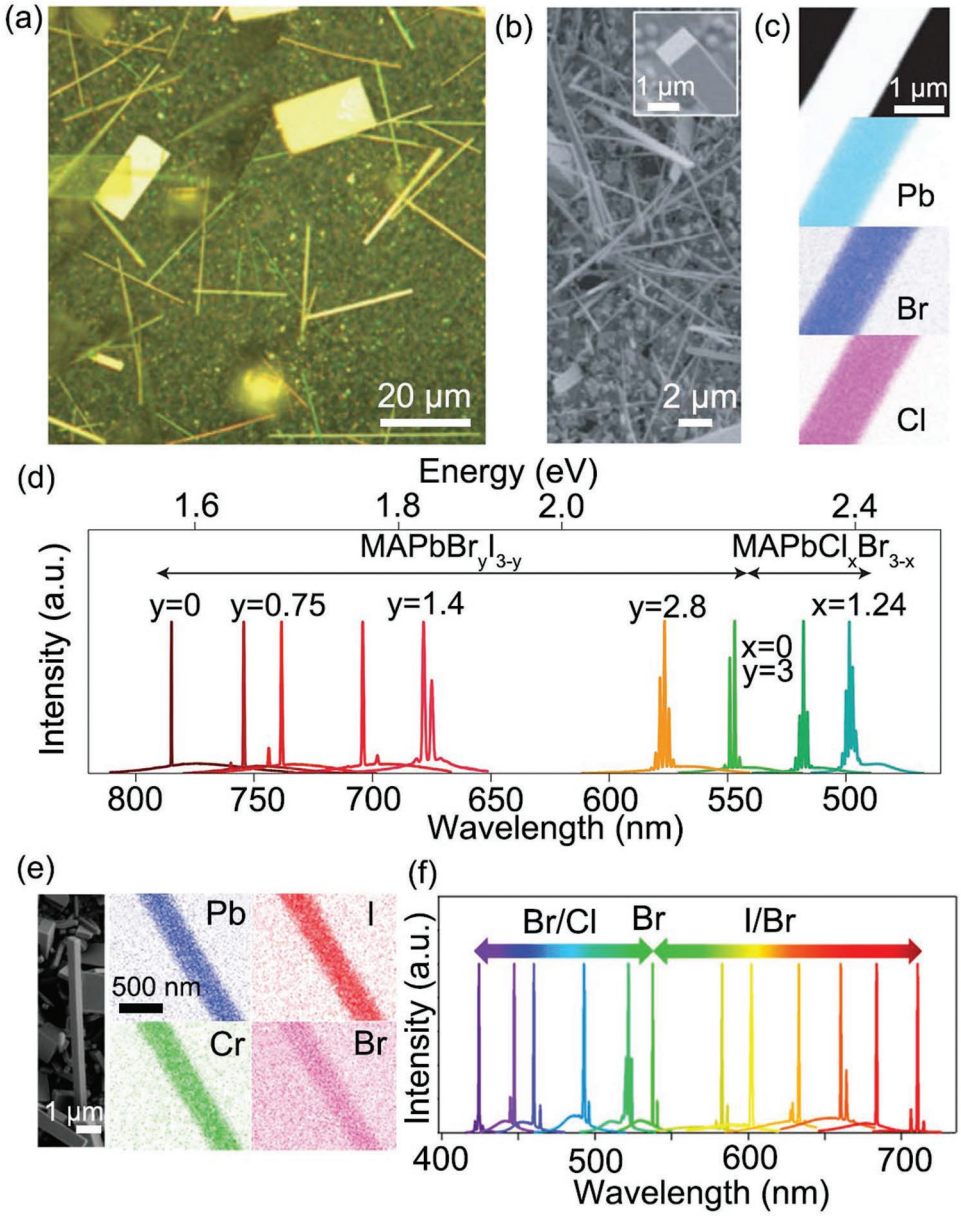

Figure 5. Lasing wavelength tuning based on 1D lead halide perovskite nanostructures. a) Optical and b) SEM images of $MAPbCl_{1.24}Br_{1.76}$ nanostructures. c) Typical SEM image (top) of an individual $MAPbCl_{1.24}Br_{1.76}$ nanowire and the corresponding energy-dispersive X-ray spectroscopy (EDX) mapping showing the uniform elemental distribution of Pb, Cl, and Br. d) Wavelength-tunable lasing emission at room temperature from composition-varied lead halide perovskite nanowire lasers. (a–d) Reproduced with permission.[151] Copyright 2015, Springer Nature. e) Left: a SEM image of a nanowire after conversion with well-preserved morphology and rectangular flat end-facet. Right: EDX mapping of the corresponding NW shows uniform spatial distribution of Cs, Pb, Br, and I elements. f) Wavelength-tunable lasing emission at room temperature from nanowires of $CsPbX_3$ (X = Cl, Br, and I). (e,f) Reproduced with permission.[163] Copyright 2016, American Chemical Society.

B is Pb^{2+} or Sn^{2+}, and X is Cl^-, Br^-, or I^-).[56,82,139] Very recently, novel lead halide perovskite nanomaterials including quantum dots (0D),[148–150] nanowires (1D),[138,145,151,152] and nanoplatelets (2D)[153–156] have been synthesized via colloidal methods,[84] solution growth methods,[157] and vapor deposition methods.[158] Owing to the dynamic nature of the halide perovskite lattice, a great number of material combinations can be easily achieved, which is superior to traditional III–V or II–VI semiconductor materials. Thus, metal halide perovskites represent a promising candidate for the tuning of bandgaps, conductivities, mobilities, and other properties.

As shown in **Figure 5**, lasing in a perovskite nanowire synthesized through a solution method was reported for the first time.[151] The perovskite nanowires were grown by exposing a lead acetate film to a solution of MA halide salt, which is a surface-initiated solution growth strategy. This method involves the transfer of well-dispersed perovskite nanowires through a dry contact process from the growth surface to another substrate,

© 2019 WILEY-VCH Verlag GmbH & Co. KGaA, Weinheim

which are then pumped optically to lase at room temperature in a dry N_2 atmosphere. Based on the long carrier lifetimes and low nonradiative recombination rates arising from their good crystalline quality, these nanowire lasers possess superior cavity characteristics and extremely low thresholds. Based on multiple nanowires, they realized widely tunable lasing wavelengths at room temperature using multiple nanowire with different composition. The solution method is more controllable compared with method using high-temperature or vacuum synthesis processes.

Although the emission wavelength tunability demonstrated in perovskite materials is an attractive optical property for MNLs, lead halide perovskites have well-known intrinsic instability issues.[159,160] A type of cesium lead halide perovskite[57,84,152,157,161–163] has emerged as an improved and robust alternative with emission wavelength tunability ranges of over 100 nm.[157] FA-based perovskite nanowires[163–167] are another kind of materials with improved photostabilities, higher Q factors of ~2000, and wider wavelength tunabilities than those of MA-based perovskites nanowires.[166]

Besides nanowires (1D), quantum dot (0D) suspensions with long carrier lifetimes exhibit both size- and composition-tunable bandgap energies from 400 to 700 nm,[168] covering the entire visible spectral region with narrow and bright PL emission. In another work, $CsPbX_3$ self-assembled nanoplatelets (2D)[169] with thicknesses of only a few integer numbers of perovskite unit cells also exhibited clear quantum size effects,[170] with different emission peaks at fixed wavelengths.

Very recently, some efforts have been taken into the spatially controlled[171,172] or composition-graded[173] halide perovskites MNL, which are promising to play a key role in their applications in micro/nanoscale photonic devices. By postsynthetic and control of the optical properties of lead halide perovskites, including wavelengths of absorption, PL, and lasing, Song and co-workers realized the blueshifted wavelength range of around 50 nm.[171] Combined with nanofabrication, the anion-exchange chemical techniques have been proved to be very useful in precisely controlling the spatial patterns of multicolor $CsPbX_3$ (X = Cl, Br, I, or alloy of two halides) NWs in Yang's work.[172] Furthermore, the direct synthesis of $CsPbBr_xI_{3-x}$ NWs along which the composition is graded with an increased Br/I from the center to the ends has been reported through the approach of vapor-phase epitaxial growth.[173] Based on this kind of NWs, dual-color lasing (at 521 and 556 nm) from single NWs is realized. In the future, halide perovskite-based MNLs face the challenge of precisely and continuously lasing wavelength tuning in single micro/nanostructures.

2.3. 2D Transition Metal Dichalcogenides

As an important member of the low-dimensional optical material family,[174] 2D materials own huge potential in a great number of applications such as phototransistors,[175] p-n diodes,[176] and light-emitting diodes.[177] In the past several years, 2D TMDCs also have provided an exciting opportunity for the design of wavelength-tunable MNLs with their optical, electronic, and spintronic properties.[64,178–183] Compared with the bulk material, a freestanding MoS_2 monolayer strongly emits light with a dramatic increase in luminescence quantum efficiency of more than 10^4-fold.[64]

Between 2014 and 2015, the synthesis of large-area continuous films of 2D $MoS_{2(1-x)}Se_{2x}$ semiconductor alloys[87] was achieved based on a vapor phase method.[184,185] Controllable selenization processes were applied to preprepared sulfurized monolayers (e.g., MoS_2) for accurate substitution of S atom with Se atom by simply adjusting the temperature. This kind of alloyed material represents an attractive step in the pursuit of practical bandgap engineering applications. The bandgap PL of as-grown $MoS_{2(1-x)}Se_{2x}$ monolayers can be continuously tuned from 1.86 eV (where $x = 0.00$) to 1.55 eV (where $x = 1.00$).[87,88] Another method to attain bandgap-tunable alloyed monolayers is mechanical exfoliation of bulk crystal alloys. For instance, by using Scotch tape, a $Mo_{1-x}W_xSe_2$ monolayer and few-layer alloy samples were mechanically exfoliated from bulk $Mo_{1-x}W_xSe_2$ crystals on a SiO_2/Si (300 nm thick oxide) substrate.[89]

For atomically thin TMDC materials, the gain provided by the monolayer cannot satisfy the lasing threshold condition under the cavity itself whose Q factor is too low and the confinement factor is too weak to form efficient lasing oscillation. As recently reported, a higher Q factor microcavity such as a photonic crystal[104,186] or whispering gallery mode[187] resonators can be combined with larger confinement factors arising from the cavity geometries containing an embedded TMDC gain material instead of relying on weak evanescent coupling (**Figure 6**). This leads to a newly designed laser rate-equation theory[188] that is appropriate for describing TMDC nanolasing processes.

Therefore, due to strong excitonic emission and high quantum efficiency, the 2D monolayer TMDCs have the huge potential to be the ideal gain media for MNLs. Besides, precisely tuning the bandgap is of great significance for expanding the application of TMDC materials. Such alloyed materials with multiple element combination offer a unique opportunity for wavelength-tunable MNL. Even though, currently, there is no tunable MNL based on TMDC materials, hybrid structures with high Q factors and strong confinement factors may allow for the realization of wavelength-tunable MNLs based on 2D TMDCs.

3. Cavity Design for Wavelength Tuning

Nanowires, an important part of the micro/nanostructure library, are favored for their flexible structures, which are convenient for forming various geometries with modified performances. One typical route to reforming the cavities of preexisting nanowires is to loop them as a ring resonator or looped mirror, etc. The first case of a ring nanowire laser was demonstrated with GaN nanowire,[189] where both ends of the nanowire were bent by 90° to overlap with each other evanescently, as shown in **Figure 7**a–d. Though ring resonator nanowire lasers have many advantages, their tunable wavelength range is limited by the inherent gain profile of the medium, and their mechanical instability cannot be ignored. The latter has been improved by splicing the ends of the nanowires together melting a short polystyrene nanowire at the overlapping region, which also enhances the cavity resonance by lowering the coupling loss.[190]

© 2019 WILEY-VCH Verlag GmbH & Co. KGaA, Weinheim

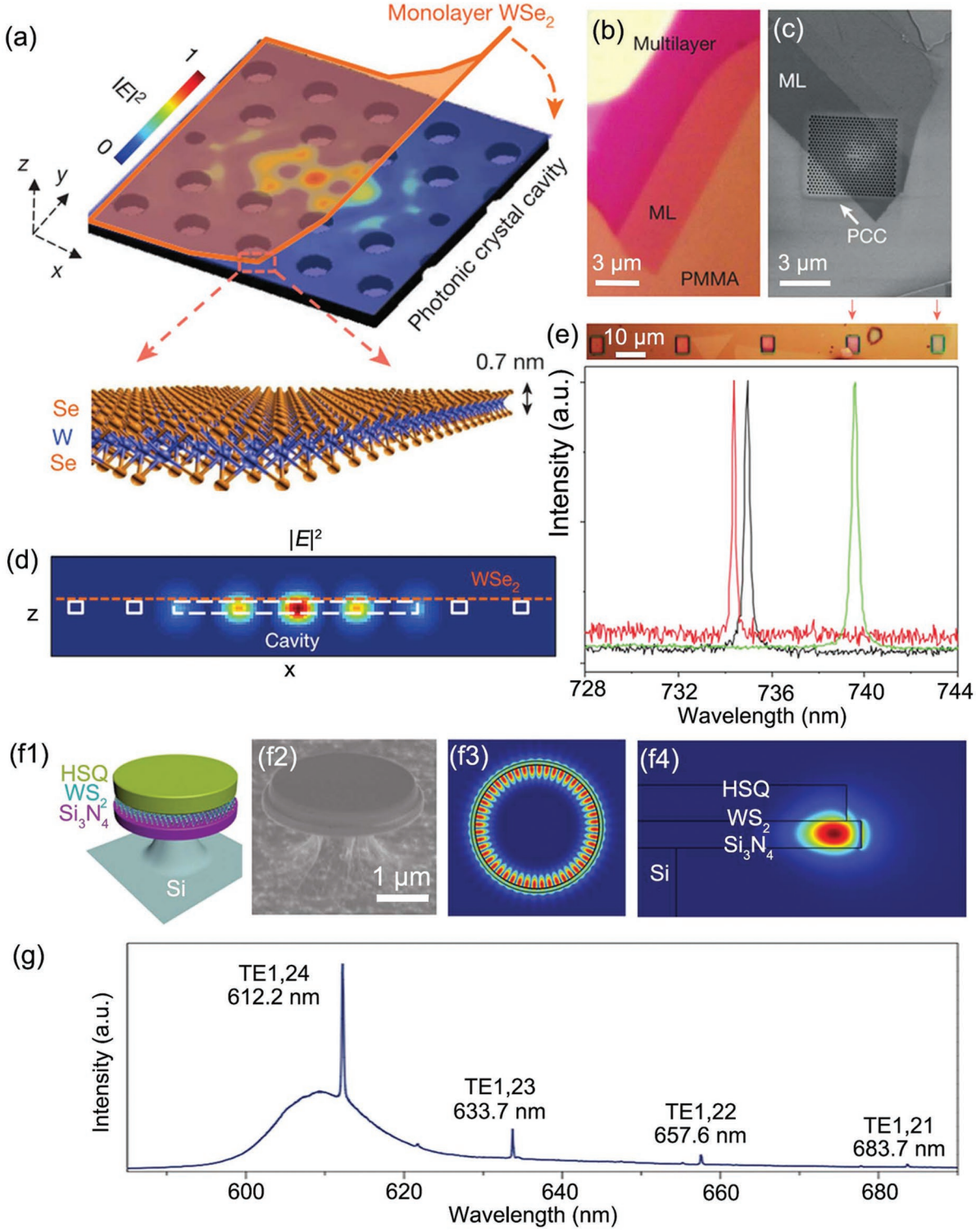

Figure 6. Hybrid-structure MNLs based on TMDCs combined with photonic-crystal[104] and microdisk resonators.[187] a) Scheme of the device architecture, where the electric field profile (in-plane, *x*–*y*) of the fundamental cavity mode (pristine cavity before WSe_2 transfer) is embedded as the color plot. Inset: cartoon of the atomic structure of monolayer WSe_2. b) Optical image of monolayer WSe_2 on PMMA before transfer. c) SEM image of the hybrid device. d) Cross-section electric field intensity profile of the fundamental mode. e) Reproducibility and scalability of the 2D nanolasers. (a–e) Reproduced with permission.[104] Copyright 2015, Springer Nature. f1–4) From left to right: schematic image of a monolayer WS_2 microdisk laser, SEM image, top view of the simulated electric field distribution of the $TE_{1,24}$ resonance, cross-sectional view of the calculated electric field distribution of the $TE_{1,24}$ resonance. g) Experimental PL spectrum taken at 10 K when the pump intensity is above lasing threshold, showing whispering gallery modes at 612.2, 633.7, 657.6, and 683.7 nm. (f,g) Reproduced with permission.[187] Copyright 2015, Springer Nature.

© 2019 WILEY-VCH Verlag GmbH & Co. KGaA, Weinheim

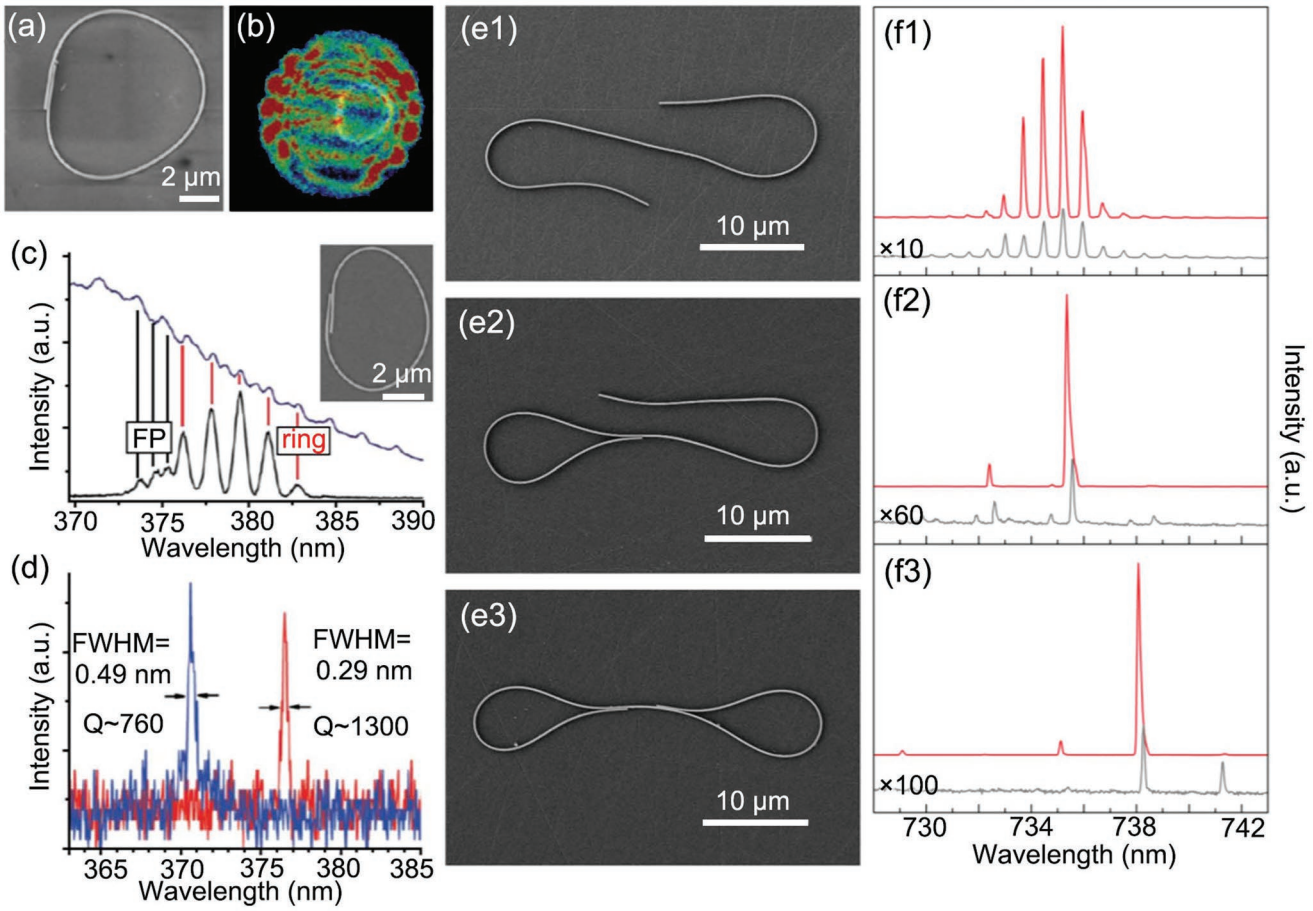

Figure 7. Wavelength tuning based on looping pure single nanowires. a) SEM of a ring structure established by a single GaN nanowire. b) A CCD image of laser mode interference scattering from end-facets of the ring in (a). c) Comparison of lasing mode structure (black) and PL (blue) from a ring resonator with a partially detached facet couple. Lasing preferentially occurs in one of the two counter-propagating resonator modes. Inset: SEM of another ring. d) Cavity *Q* factors were measured from wire and ring lasing emission spectra. (a–d) Reproduced with permission.[189] Copyright 2006, American Physical Society. e1–3) From top to bottom, SEM images of single-nanowire structures without loop mirror, with on loop mirror and with double loop mirrors. f1–3) Lasing spectra of single-nanowire structures in (e), respectively. (e,f) Reproduced with permission.[191] Copyright 2011, American Chemical Society.

In addition to wavelength tunability, looped nanowire lasers have another advantage in their facile approach to mode selection. Figure 7e shows the folding of two ends of a CdSe nanowire by micromanipulation to form loop mirrors. With this nanowire loop and coupled resonant cavities, a single-mode laser can be readily generated by means of Vernier effect, a common mode-selection technique.[191] Through adjusting the size of the flexible loop structure by micromanipulation, the wavelength of the single-mode nanowire laser can be tuned from 735.36 to 738.08 nm (Figure 7f). Another work reported the formation of a cleaved coupled cavity[98] fabricated by cutting a single GaN nanowire by focused ion beam (FIB) and forming two Fabry–Pérot cavities axially. The output of this nanolaser can be tuned by changing the cleave position and width.

Other cavity-design approaches to wavelength tunability have also been explored. Based on this factor, one effective approach to switching the lasing wavelength is to combine multiple cavities together. For example, Ma et al.[192] proposed a kind of plasmonic circuit integrating five independently modulated multiwavelength plasmon lasers on a chip. Several parallel-separated silver strips crossed a CdS nanobelt with a 5-nm-thick magnesium fluoride gap layer between them. The CdS nanobelt, whose width narrowed down gradually along its length, acted simultaneously as a waveguide and a gain medium. Naturally, the cross-sectional areas of these squared-shaped cavities changed along the length of the CdS nanobelt, and modulated the resonant conditions and the emission wavelength. Owing to the discrete changes, the wavelength tunability is evidently noncontinuous and low-repeatability, with a demonstrated spectral tuning range of 12 nm.

Refractive index is also another key factor that influences the oscillating longitudinal modes. Recently, tuning lattice plasmon modes by changing refractive index has been reported both in static (**Figure 8**a) and dynamic real-time (Figure 8d,e) wavelength tuning.[100] In this work, optically pumped arrays of gold nanoparticles provide a plasmonic resonator surrounded by the gain dye molecules. Dissolving IR-140 dye in several kinds of solvents with varied refractive indices (0.08 in difference) leads to the slight shift of lasing wavelengths from 853 to 896 nm in

© 2019 WILEY-VCH Verlag GmbH & Co. KGaA, Weinheim

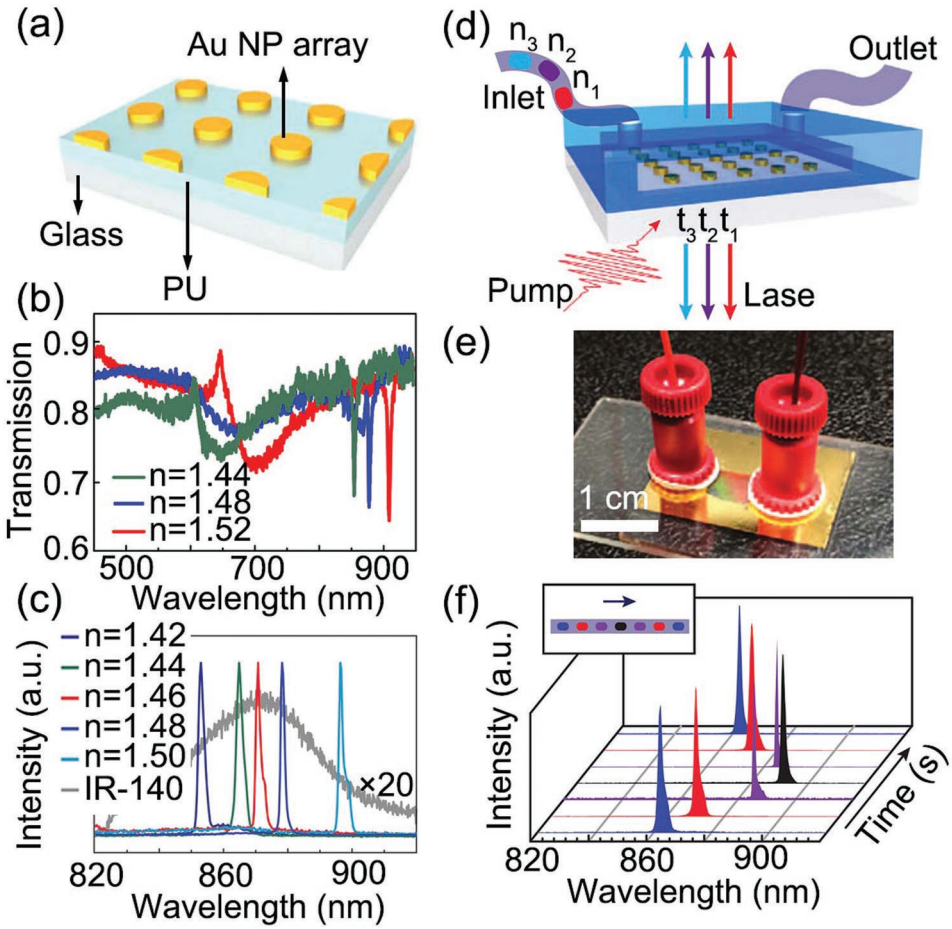

Figure 8. Lasing wavelength tuning due to refractive index changing. a) Scheme of Au nanoparticles arrays on a near-atomically flat PU substrate and a transparent glass substrate. b) Transmission experiments of Au nanoparticles in different dielectric environments (n = 1.44, 1.48, and 1.52). c) Experimental results of lasing emission from Au nanoparticles arrays embedded in different index environments from n = 1.42 to n = 1.50. The gray curve represents the PL of IR-140. d) Scheme of the dynamic laser and e) photograph of the device. f) IR-140 dye molecules were dissolved in DMSO (blue), DMSO:BA = 2:1 (red), DMSO:BA = 1:2 (purple), and BA (black). PU: polyurethane, DMSO: dimethyl sulfoxide, BA: benzyl alcohol. Reproduced with permission.[100] Copyright 2015, Springer Nature.

static tuning (Figure 8b,c) and from 862 to 891 nm in dynamic tuning (Figure 8f).

4. Wavelength Tuning from Combination of Cavity Design and Bandgap Tuning

4.1. Combination of Cavity Design and Single Micro/Nanostructures

In different combinations of gain material and cavity design, several approaches realizing wavelength-tunable MNLs based on single devices have been demonstrated.[101,193] One strategy for achieving wavelength-tunable lasers based on single micro/nanostructures relies on the intrinsic self-absorption of the gain medium at the Urbach tail states to tailor the nanowire cavity lasing wavelength. In undoped polar semiconductors, the density of states has been demonstrated to extend from the band edge into the bandgap due to the fluctuation in electronic energy bands resulting from exciton–phonon coupling.[194–196] Optical transitions with lower energies result in an exponential tail near the optical absorption edge known as the Urbach tail. This effect increases in semiconductor nanowires due to much stronger exciton–phonon coupling than that of their bulk counterparts.[197] In 1D model nanostructure systems such as pure CdS and CdSe nanowires, band-tail absorption in longer nanowires results in a redshift of the wavelength of oscillating light. This approach has been demonstrated in both pure nanowires[101,198] and allows for excellent wavelength tunability and selectivity covering more than several tens of nanometers with almost unchanged cavity quality (**Figure 9**). In particular, Li et al. demonstrated wide-wavelength-tunable lasers (40 nm tuning range from 746 to 706 nm) using a bend-to-facture method to cut a 289-µm-long CdSe nanowire step by step.[101] A recent work[193] also demonstrated a wavelength-tunable nanolaser (26 nm tuning range from 491 to 465 nm) by adjustment of the length of the CdS nanowire from 26.4 down to 5.2 µm.

© 2019 WILEY-VCH Verlag GmbH & Co. KGaA, Weinheim

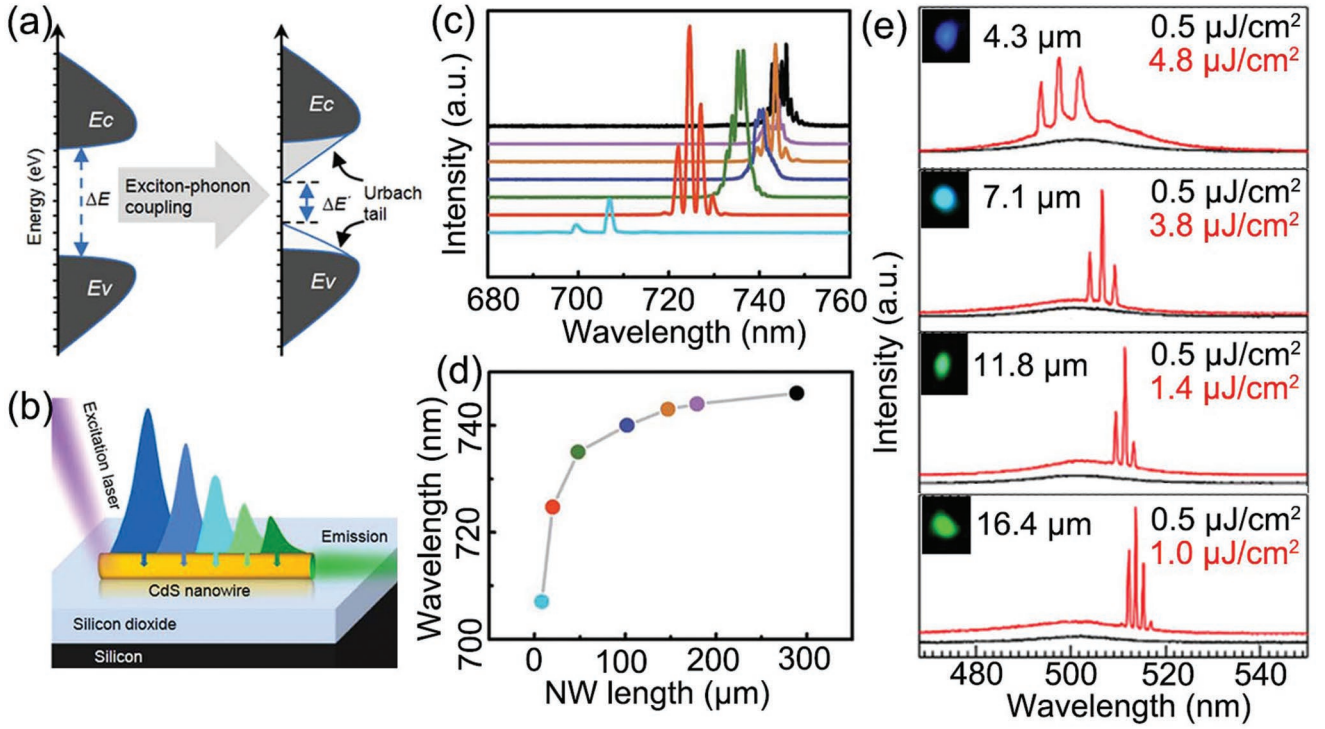

Figure 9. Wavelength tuning based on Urbach tail effect. a,b) Schematics of the Urbach tails at the band edges and the length-dependent lasing wavelength selections for pure semiconductor nanowires.[198] c) Lasing spectra from a single CdSe nanowire with different lengths under the same pump beam size and intensity. d) Nanowire length dependent dominant lasing peak wavelength. (c,d) Reproduced with permission.[101] Copyright 2013, Wiley-VCH. e) Lasing spectra from four CdS nanowires with different lengths of 4.3, 7.1, 11.8, and 16.4 μm, respectively. The insets are CCD images of colorful spots from the four CdS nanowires undergoing lasing. (a,b,e) Reproduced with permission.[198] Copyright 2013, American Chemical Society.

Over the past decade, much attention has focused on the realization of wavelength-tunable MNLs based on composition-graded nanostructures by combination with oscillating cavity design to overcome asymmetric light absorption. As a result of asymmetric light propagation (**Figure 10**) in composition-graded semiconductor nanowires,[76,199,200] for a single composition-graded nanostructure, the lasing wavelength is entirely determined by the narrowest bandgap of the whole structure.[102] The goal of designing a new resonator is to eliminate the negative effect resulting from the asymmetric absorption in such newly developed materials.

Several approaches to cavity design combined with composition-graded 1D materials have been reported.[102,124,127,201] Liu et al.[127] demonstrated dynamic color tuning in a wide spectrum range in a single CdSSe nanowire. By looping the wide-bandgap end of the alloy nanowire (400 μm in length) through nanomanipulation, two largely independent laser cavities (one ring cavity with 15 μm diameter and one Fabry–Pérot cavity) are formed, respectively. Two lasing wavelengths are obtained from the nanowire laser at 637 and 530 nm, respectively. Aside from that, the dynamic control on the pumping power enables a color tuning of the overall output of this nanolaser from green to red. Even though the wavelength of this novel dual-colored laser is difficult to be tuned repeatedly and precisely, it still possesses the potential for a white-color laser.

Multicolor lasers have also been achieved via utilization of scattering from morphological in situ generated defects on CdSSe composition-graded nanoribbons.[124] In situ generated defects act as scattering center inside the nanowire and hence form multiple cavities with randomly distributed position and volume. These randomly distributed nanocavities then can react differently to external pump and form multiwavelength lasers covering from 578 to 640 nm.

As shown in **Figure 11**a–c, since the lasing wavelength of composition-graded nanostructures is well-defined by the narrow-end bandgap, Yang et al. demonstrated that cutting the narrow bandgap end of a 450-nm-diameter CdSSe nanowire from 435 to 8 μm could enable the lasing wavelength of the nanowire laser to be shifted from 636 to 517 nm (covering a 119 nm spectral range).[102] In addition, shortening the nanowire length not only alters the asymmetric absorption but also broadens the free spectral range, hence eventually a single-longitudinal-mode laser is realized.

As shown in Figure 11d,e, the most recent strategy for tuning the lasing wavelength of composition-graded micro/nanostructures relies on a new cavity design that separates the gain material and the optical resonator.[201] The single GaN/InGaN core–shell microrod with a length of 10 μm acts as a hybrid cavity. Light oscillates in the GaN core with limited asymmetrical absorption while amplifies by the InGaN shell gain media via evanescent interaction. The emitted lasing wavelength depends

© 2019 WILEY-VCH Verlag GmbH & Co. KGaA, Weinheim

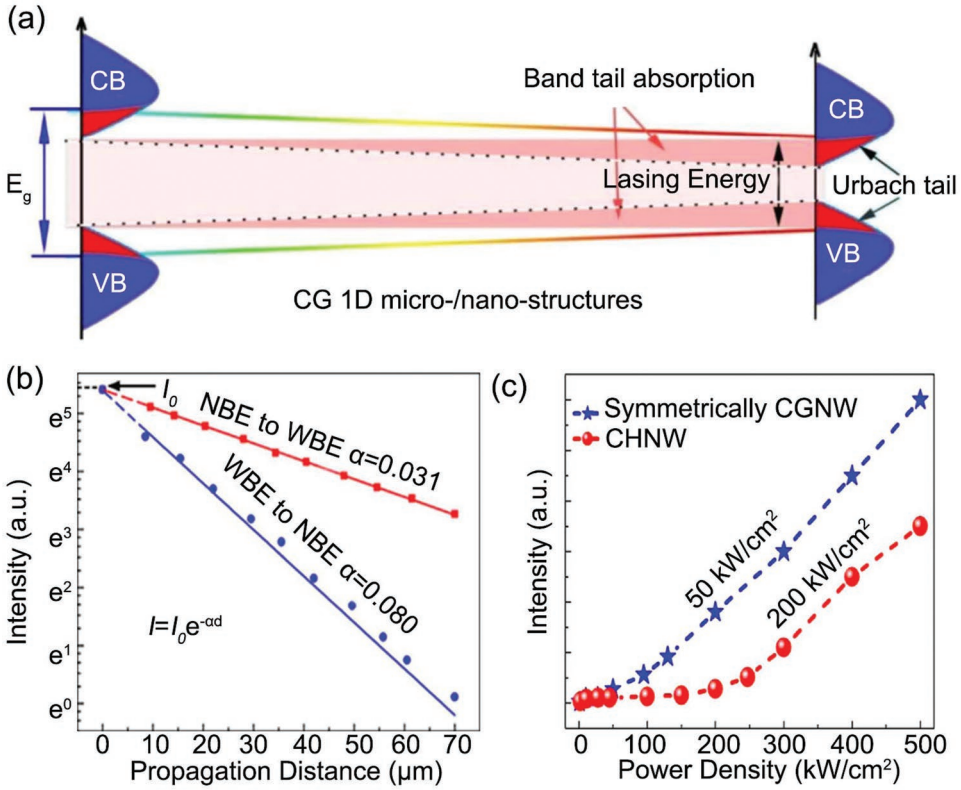

Figure 10. The asymmetric absorption in composition-graded (CG) 1D micro/nanostructures. a) Band diagram of bandgap-graded nanowires. Reproduced with permission.[102] Copyright 2014, American Chemical Society. b) Propagation distance-dependent PL integrated intensity at WBE and NBE, respectively. Reproduced with permission.[200] Copyright 2012, Springer Nature. c) Pumping power-dependent emission intensity for symmetrically CGNW (blue pentagrams) and CdS_xSe_{1-x} alloy CHNW (red spheres), respectively. Reproduced with permission.[199] Copyright 2014, American Chemical Society. CB, conduction band; VB, valence band; NBE, narrow-bandgap end; WBE, wide-bandgap end; CGNW, composition-graded nanowire; CHNW, composition-homogeneous nanowire.

on the external pump position. Using this method, controllable lasing wavelengths from 372 to 408 nm has been demonstrated with high repeatability.

4.2. Combination of Cavity Design and Burstein–Moss Effect

The Burstein–Moss effect proposed independently by Burstein[202] and Moss[203] in their research on InSb describes the evident blueshift of a semiconductor bandgap[106] arising from the Pauli exclusion principle, which is commonly utilized to tune the bandgap of traditional semiconductors. However, this spectral shift is limited in undoped semiconductors, indicating the Burstein–Moss effect is very weak.[198] In 2013, Liu et al. proposed that the Burstein–Moss effect can be strengthened when combined with SPPs. Due to the coupling between the CdS excitons and SPP in the hybrid devices with SiO_2 layers, the carriers are confined in subwavelength modes which resides at the interface, resulting in a high carrier concentration and thus an enhancement of the Burstein–Moss effect. As shown in **Figure 12**, by decreasing the thickness of SiO_2 intermediate layer from 100 to 5 nm, the interaction between the SPP and the excitons becomes stronger, which allows for the blueshift of the emission wavelength from 504 to 483 nm.[204]

5. Operating Environmental Condition Induced Lasing Wavelength Tuning

Besides the bandgap tuning and cavity design, the lasing wavelength of MNLs can also be tuned by the operating environment conditions including temperature,[205,206] pressure,[126] and strain.[207]

As shown in **Figure 13**a–c, as the lattice temperature increases from 10 to 285 K,[205] the bandgap of the nanowire reduces, thereby redshifting the dominant lasing energy in GaAs nanowires from 1.50 to 1.39 eV. Furthermore, the single mode becomes multiple modes when the lattice temperature rises above 220 K, which originates from the temperature-induced peak gain reduction, and the gain spectrum broadening that is comparable with the free spectral range.

As the equilibrium branching ratio between free charges and bound excitons varies with temperature, Xing et al.[206] reported lasing wavelength tuning in highly crystalline $MAPbI_3$ nanowires based on Varshni effect. By decreasing the experimental temperature from 300 to 80 K, the lasing wavelength of $MAPbI_3$ nanowires redshifts from 780 to 795 nm.

A recently work[28] reported that a SPP nanolaser operates steadily over a wide temperature range from 77 to 353 K with outputs redshifted from 372 to 386 nm due to the Varshni trend

© 2019 WILEY-VCH Verlag GmbH & Co. KGaA, Weinheim

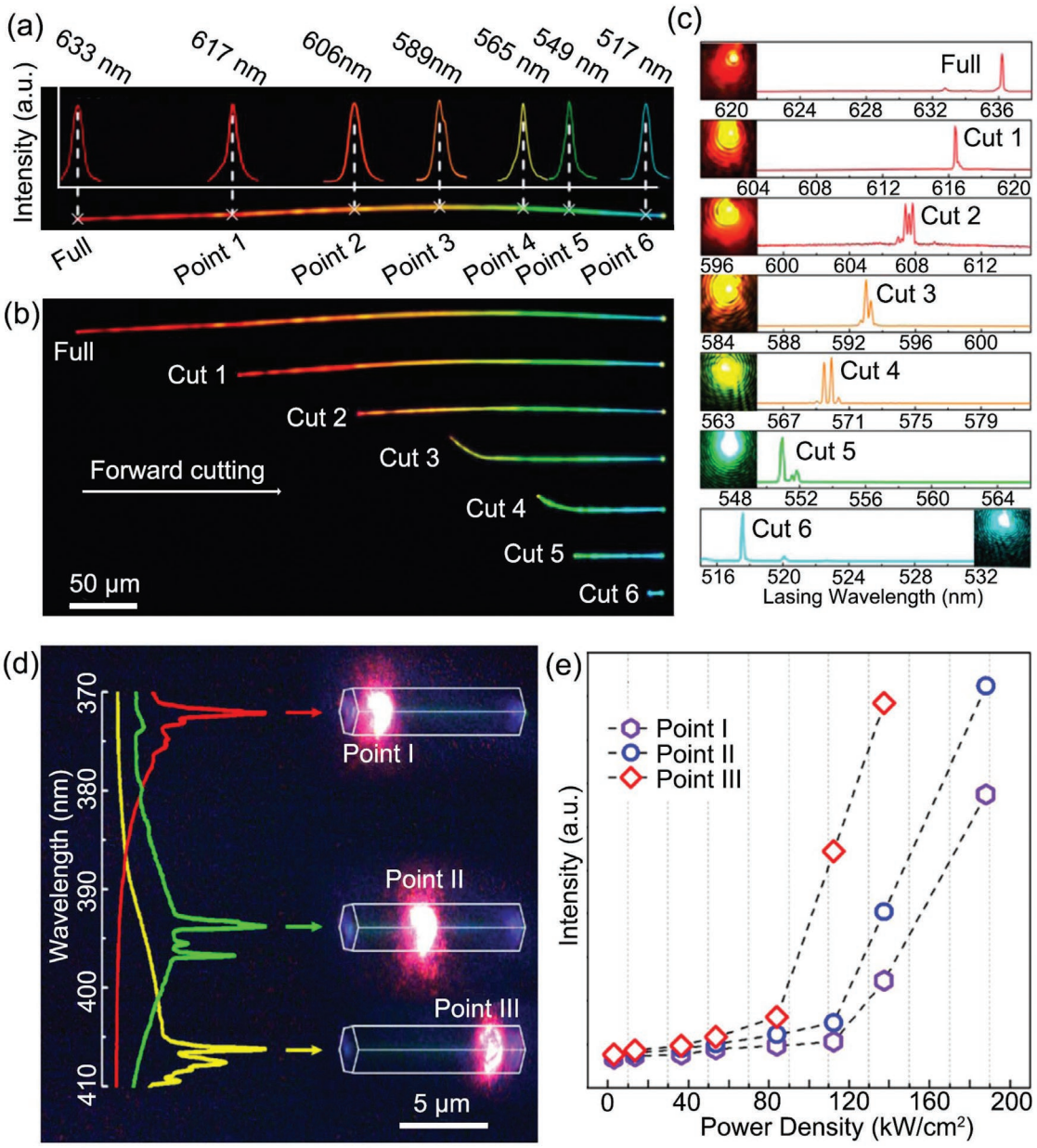

Figure 11. Continuously wavelength tuning in the new cavity design combined with the composition-graded micro/nanostructures. a) CCD image of a bandgap-graded nanowire with six cut points determined by localized PL spectra. b) CCD images of the nanowire from full to being cut at point 6 sequentially. c) Lasing spectra obtained from NW full to cut 6 in (b) inserted with colorful spots of CCD images of the end lasing emission from each nanowire. (a–c) Reproduced with permission.[102] Copyright 2014, American Chemical Society. d) Lasing spectrum and CCD images of different excited points in a single GaN/InGaN core–shell microrod. e) The lasing threshold at different excitation points (different lasing wavelengths). (d,e) Reproduced with permission.[201] Copyright 2017, American Chemical Society.

of the ZnO exciton. Furthermore, a decrease in lasing threshold for a ZnO/Al structure has been demonstrated. This easy-to-fabricate hybrid structure provides higher waveguide confinement factor comparing with $ZnO/Al_2O_3/Al$ structure and thus sufficient to confine the light energy and overcome the higher propagation loss.[28]

High hydrostatic pressure has also been explored in the exploration of wavelength-tunable MNLs by utilization of a diamond anvil cell with silicone oil as a hydrostatic pressure-transmitting medium. For example, experimental results on GaN nanowires (Figure 13d,e)[126] indicated that the lasing wavelength in GaN nanowires can blueshift from ≈367 to 337 nm when the applied pressures vary from ambient pressure to ≈7 GPa and beyond. GaN materials possess enhanced pressure coefficients compared with their bulk counterparts.[207,208] The above-mentioned lasing wavelength shift originates from the broadening of the nanowire's bandgap when the lattice is squeezed under pressure.

© 2019 WILEY-VCH Verlag GmbH & Co. KGaA, Weinheim

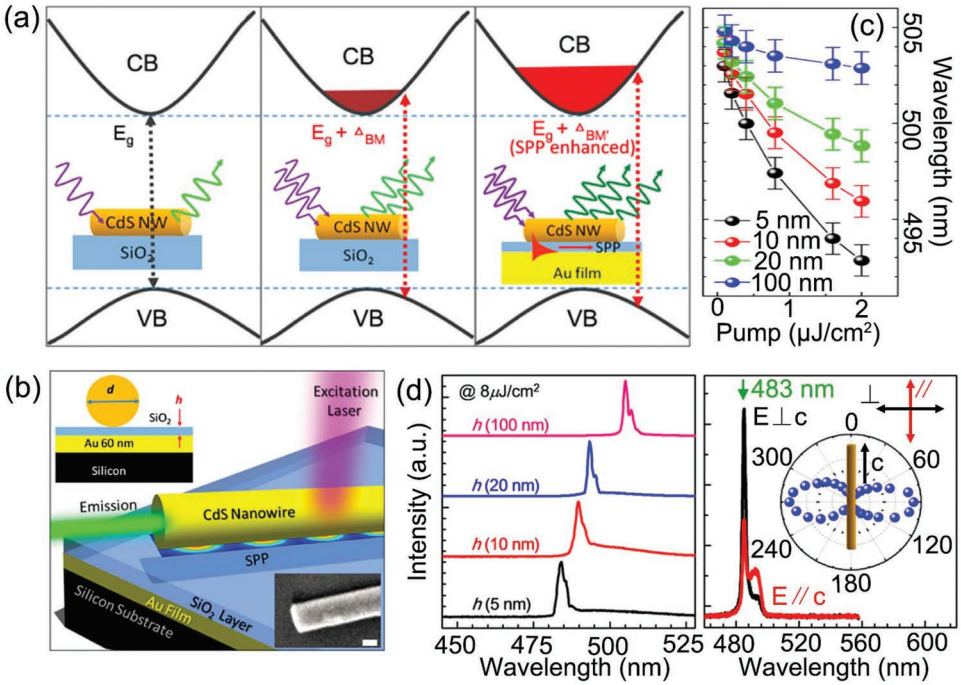

Figure 12. Bandgap tuning by changing the BM effect enhanced by SPP. a) Schematics of various effects on the bandgap energy of pure semiconductors nanowires. b) A schematic of the NW laser devices. Inset (bottom right corner) is SEM image of a typical single CdS NW on a 5-nm-thick gold film. The scale bar is 100 nm. c) The emission peak positions of four devices with different heights of SiO_2 substrates. d) Lasing spectra from the four devices and the results of polarization-dependent experiments (*c*-axis is along the NW length). Reproduced with permission.[204] Copyright 2013, American Chemical Society.

In 2007 and 2010, Wang et al. proposed the two methods utilizing piezotronics and piezophototronics with the coupling of electric, optical, and stress fields based on wurtzite-structural semiconductors by applying a strain.[209–212] Very recently, the ability to modulate the optical bandgap of wurtzite-structural ZnO via external mechanical pressure and tensile strain has drawn significant attention.[98–100] However, the redshift of PL spectrum induced by tensile strain is too small to modulate the lasing competition. Thus, in 2018, Lu et al.[213] demonstrated that variation of external tensile strain induces the polarization effect which leads to a change in the refractive index. Due to this piezoelectric polarization effect of ZnO under tensile strain, the increased refractive index changes the resonant condition of lasing wavelength which appears a redshift of emission peaks (Figure 13f,g). The ultranarrow line width of the ZnO lasing mode compared to that of PL modes drastically improves the sensitivity of strain detection, which results in extremely sensitive wavelength tuning induced by tensile strain. Moreover, the tunable spectral range can cover less than 10 nm.

6. Conclusion and Future Prospects

All of the discussed efforts in this review have aimed at applications in a variety of fields. We have briefly discussed several strategies that have been utilized for realizing wavelength tunabilities in MNLs. Here, we summarized some typical results and references in Table 1. Owing to their novel features in light emission efficiencies, high gain coefficients, and strong confinement factors, MNLs are the best candidate to meet the requirements of low cost, low power consumption, and good compatibility for more practical applications.

One possible practical application of wavelength-tunable MNLs is on-chip integrated optical components from lasing sources and amplifiers to modulators,[4,214–216] high-capacity wavelength division multiplexed transmission and photonic switch,[217,218] which require low costs, low power consumption, and miniaturized physical sizes. In solid-state lighting, illumination and displays still require low-cost and high-efficiency light sources, such as white-light-emitting diodes and portable colorful laser diodes with long lifetimes and stable performances. Additionally, continuously wavelength-variable lasers are still necessary in spectral analysis.[219] Semiconductor MNLs with wavelength tunability can be very useful for the developing integrated air pollutants detector.[220] On the other hand, SPP MNLs with biochemical compatibility are also good choices as probe for biological applications.[221,222] Furthermore, wavelength-tunable MNLs have potential for pushing super-resolution forward to full spectral super-resolution imaging.[223,224]

In this review, we have mainly focused on two main routes—bandgap tuning and cavity design in the field of wavelength-tunable nanolaser researches (Table 1). The former drives a large number of strategies toward lasing wavelength tunability. This approach presents the possibility of the widest spectral dynamic tuning range up to now. While the cavity design, including cutting off nanowires, cleaving nanostructures, looping nanowires, and separating gain and cavity, allows for fine-tuning of lasing wavelength and is also often combined with the bandgap tuning.

© 2019 WILEY-VCH Verlag GmbH & Co. KGaA, Weinheim

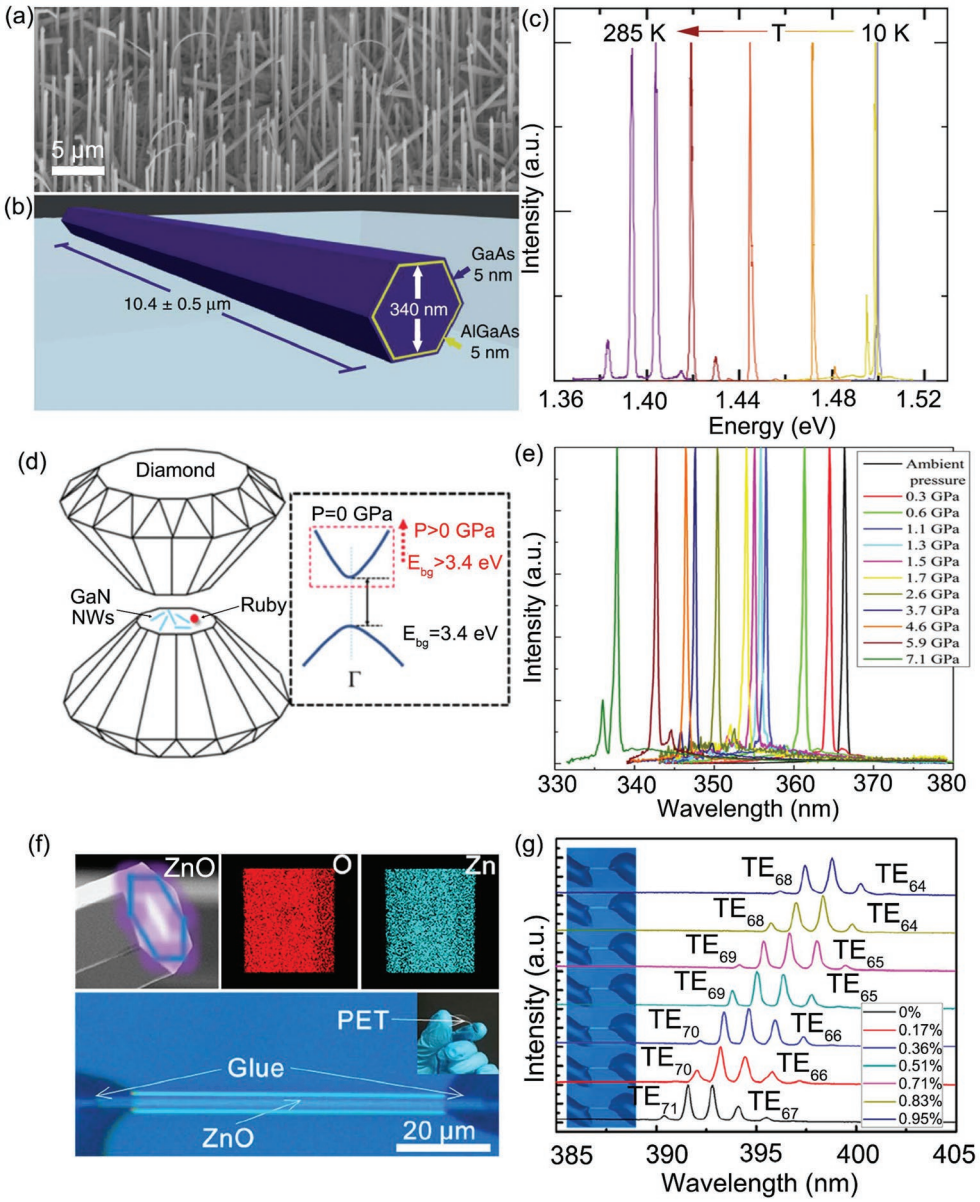

Figure 13. Bandgap tuning due to temperature and pressure changing. a) A SEM image of the as-grown core–shell GaAs-$Al_{0.25}Ga_{0.75}As$ nanowires. b) Schematic representation of a nanowire transferred onto a glass microscope slide showing the active GaAs core with a nominal diameter of 340 nm, the 5-nm-thick AlGaAs diffusion barrier, and 5 nm thick surface capping layer. c) Temperature-dependent emission spectra (normalized intensity) recorded from a single nanowire pumped above threshold at 10, 50, 110, 170, 220, and 285 K. (a–c) Reproduced with permission.[205] Copyright 2013, Springer Nature. d) Schematic of GaN nanowires under hydrostatic pressure applied by a diamond anvil cell consists of two diamonds facing each other. Ruby microspheres are placed inside the diamond anvil cell to monitor the pressure. e) Wavelength-tunable lasing emission from a single GaN nanowire at different pressures.[126] Copyright 2015, Royal Society of Chemistry. f) Upper: Zn and O element mapping and a SEM image of single ZnO microwire cross section. Below: Optical image of single ZnO microwire fixed on the flexible PET substrate; inset, optical image of PET. g) Lasing spectra of ZnO microwire under different degrees of bending inserted with optical images of the sample. (d–g) Reproduced with permission.[213] Copyright 2018, American Chemical Society.

Besides, the modulation of environment conditions such as temperature, pressure, and strain enables the excellent repeatability in wavelength tuning. Thus, as the wavelength-tunable MNLs evolve, key parameters such as spectral tuning range and resolution, repeatability, device integration, and miniaturization must also be enhanced by a combination of the above methods for new generations of MNLs development.

Acknowledgements

This work was supported by the National Natural Science Foundation of China (Nos. 62822510, 61735017, and 51672245), the National Key Basic Research Program of China (No. 2015CB352003), the Zhejiang Provincial Natural Science of China (No. R17F050003), the Fundamental Research Funds for the Central Universities, and the Program for Zhejiang Leading Team of S&T Innovation. M.-H.Z. contributed to

 © 2019 WILEY-VCH Verlag GmbH & Co. KGaA, Weinheim

writing and finalizing the paper. C.P., Y.Z., J.T., and S.U. reviewed the paper. Y.M. and Q.Y. supervised the project.

Conflict of Interest

The authors declare no conflict of interest.

Keywords

bandgap engineering, micro/nanolasers, nanocavity design, wavelength tuning

Received: February 15, 2019
Revised: May 9, 2019
Published online: June 19, 2019

[1] T. H. Maiman, *Nature* **1960**, *187*, 493.
[2] T. P. H. Sidiropoulos, R. Röder, S. Geburt, O. Hess, S. A. Maier, C. Ronning, R. F. Oulton, *Nat. Phys.* **2014**, *10*, 870.
[3] Y. H. Chou, K. B. Hong, C. T. Chang, T. C. Chang, Z. T. Huang, P. J. Cheng, J. H. Yang, M. H. Lin, T. R. Lin, K. P. Chen, S. Gwo, T. C. Lu, *Nano Lett.* **2018**, *18*, 747.
[4] R. M. Ma, R. F. Oulton, *Nat. Nanotechnol.* **2019**, *14*, 12.
[5] S. L. McCall, A. F. J. Levi, R. E. Slusher, S. J. Pearton, R. A. Loga, *Appl. Phys. Lett.* **1992**, *60*, 289.
[6] K. J. Vahala, *Nature* **2003**, *424*, 839.
[7] P. Del'Haye, A. Schliesser, O. Arcizet, T. Wilken, R. Holzwarth, T. J. Kippenberg, *Nature* **2007**, *450*, 1214.
[8] O. Painter, R. K. Lee, A. Scherer, A. Yariv, J. D. O'Brien, P. D. Dapkus, I. Kim, *Science* **1999**, *284*, 1819.
[9] Y. Akahane, T. Asano, B.-S. Song, S. Noda, *Nature* **2003**, *425*, 944.
[10] Y. A. Vlasov, X.-Z. Bo, J. C. Sturm, D. J. Norris, *Nature* **2001**, *414*, 289.
[11] M. H. Huang, S. Mao, H. Feick, H. Yan, Y. Wu, H. Kind, E. Weber, R. Russo, P. Yang, *Science* **2001**, *292*, 1897.
[12] M. S. Gudiksen, L. J. Lauhon, J. Wang, D. C. Smith, C. M. Lieber, *Nature* **2002**, *415*, 617.
[13] X. Duan, Y. Huang, R. Agarwal, C. M. Lieber, *Nature* **2003**, *421*, 241.
[14] M. P. Nezhad, A. Simic, O. Bondarenko, B. Slutsky, A. Mizrahi, L. Feng, V. Lomakin, Y. Fainman, *Nat. Photonics* **2010**, *4*, 395.
[15] C.-Y. Lu, S. W. Chang, S. L. Chuang, T. D. Germann, D. Bimberg, *Appl. Phys. Lett.* **2010**, *96*, 251101.
[16] K. Ding, Z. C. Liu, L. J. Yin, M. T. Hill, M. J. H. Marell, P. J. van Veldhoven, R. Nöetzel, C. Z. Ning, *Phys. Rev. B* **2012**, *85*, 041301(R).
[17] K. Ding, L. Yin, M. T. Hill, Z. Liu, P. J. van Veldhoven, C. Z. Ning, *Appl. Phys. Lett.* **2013**, *102*, 041110.
[18] K. Ding, M. T. Hill, Z. C. Liu, L. J. Yin, P. J. van Veldhoven, C. Z. Ning, *Opt. Express* **2013**, *21*, 4728.
[19] Q. Gu, J. Shane, F. Vallini, B. Wingad, J. S. T. Smalley, N. C. Frateschi, Y. Fainman, *IEEE J. Quantum Electron.* **2014**, *50*, 499.
[20] S. H. Pan, Q. Gu, A. E. Amili, F. Vallini, Y. Fainman, *Optica* **2016**, *3*, 1260.
[21] E. Bermúdez-Ureña, G. Tutuncuoglu, J. Cuerda, C. L. Smith, J. Bravo-Abad, S. I. Bozhevolnyi, A. Fontcuberta i Morral, F. J. García-Vidal, R. Quidant, *Nano Lett.* **2017**, *17*, 747.
[22] Y. Lu, J. Kim, H. Chen, C. Wu, N. Dabidian, C. E. Sanders, C. Wang, M. Lu, B. Li, X. Qiu, W. Chang, L. Chen, G. Shvets, C. Shih, S. Gwo, *Science* **2012**, *337*, 450.
[23] X. Wu, Y. Xiao, C. Meng, X. Zhang, S. Yu, Y. Wang, C. Yang, X. Guo, C. Z. Ning, L. Tong, *Nano Lett.* **2013**, *13*, 5654.
[24] Q. Zhang, G. Li, X. Liu, F. Qian, Y. Li, T. C. Sum, C. M. Lieber, Q. Xiong, *Nat. Commun.* **2014**, *5*, 4953.
[25] Y. J. Lu, C. Y. Wang, J. Kim, H. Y. Chen, M. Y. Lu, Y. C. Chen, W. H. Chang, L. J. Chen, M. I. Stockman, C. K. Shih, S. Gwo, *Nano Lett.* **2014**, *14*, 4381.
[26] J. Ho, J. Tatebayashi, S. Sergent, C. F. Fong, S. Iwamoto, Y. Arakawa, *ACS Photonics* **2015**, *2*, 165.
[27] J. Ho, J. Tatebayashi, S. Sergent, C. F. Fong, Y. Ota, S. Iwamoto, Y. Arakawa, *Nano Lett.* **2016**, *16*, 2845.
[28] Y. H. Chou, Y. M. Wu, K. B. Hong, B. T. Chou, J. H. Shih, Y. C. Chung, P. Y. Chen, T. R. Lin, C. C. Lin, S. D. Lin, T. C. Lu, *Nano Lett.* **2016**, *16*, 3179.
[29] H. Yu, K. Ren, Q. Wu, J. Wang, J. Lin, Z. Wang, J. Xu, R. F. Oulton, S. Qu, P. Jin, *Nanoscale* **2016**, *8*, 19536.
[30] H. Yu, T. P. H. Sidiropoulos, W. Liu, C. Ronning, P. K. Petrov, S.-H. Oh, S. A. Maier, P. Jin, R. F. Oulton, *Adv. Opt. Mater.* **2017**, *5*, 1600856.
[31] C.-J. Lee, H. Yeh, F. Cheng, P.-H. Su, T.-H. Her, Y.-C. Chen, C.-Y. Wang, S. Gwo, S. R. Bank, C.-K. Shih, W.-H. Chang, *ACS Photonics* **2017**, *4*, 1431.
[32] S. J. P. Kress, J. Cui, P. Rohner, D. K. Kim, F. V. Antolinez, K.-A. Zaininger, S. V. Jayanti, P. Richner, K. M. McPeak, D. Poulikakos, D. J. Norris, *Sci. Adv.* **2017**, *3*, e1700688.
[33] J. Lu, M. Jiang, M. Wei, C. Xu, S. Wang, Z. Zhu, F. Qin, Z. Shi, C. Pan, *ACS Photonics* **2017**, *4*, 2419.
[34] S. Liu, B. Sheng, X. Wang, D. Dong, P. Wang, Z. Chen, T. Wang, X. Rong, D. Li, L. Yang, S. Liu, M. Li, J. Zhang, W. Ge, K. Shi, Y. Tong, B. Shen, *Appl. Phys. Lett.* **2018**, *112*, 231904.
[35] R. M. Ma, R. F. Oulton, V. J. Sorger, X. Zhang, *Laser Photonics Rev.* **2013**, *7*, 1.
[36] M. C. Gather, S. H. Yun, *Nat. Photonics* **2011**, *5*, 406.
[37] C. Genet, T. W. Ebbesen, *Nature* **2007**, *445*, 39.
[38] M. I. Stockman, *Science* **2015**, *348*, 287.
[39] J. A. Schuller, E. S. Barnard, W. Cai, Y. C. Jun, J. S. White, M. L. Brongersma, *Nat. Mater.* **2010**, *9*, 193.
[40] X. Jiang, L. Shao, S.-X. Zhang, X. Yi, J. Wiersig, L. Wang, Q. Gong, M. Lončar, L. Yang, Y.-F. Xiao, *Science* **2017**, *358*, 344.
[41] M. T. Hill, M. C. Gather, *Nat. Photonics* **2014**, *8*, 908.
[42] X. Liu, P. Xu, Y. Wu, Z. Yang, C. Meng, W. Yang, J. Li, D. Wang, X. Liu, Q. Yang, *Nano Energy* **2015**, *14*, 340.
[43] Y. Ding, Q. Yang, X. Guo, S. Wang, F. Gu, J. Fu, Q. Wan, J. Cheng, L. Tong, *Opt. Express* **2009**, *17*, 21813.
[44] F. Fan, S. Turkdogan, Z. Liu, D. Shelhammer, C. Z. Ning, *Nat. Nanotechnol.* **2015**, *10*, 796.
[45] R. Kirchain, L. Kimerling, *Nat. Photonics* **2007**, *1*, 303.
[46] J. Buus, E. J. Murphy, *J. Lightwave Technol.* **2006**, *24*, 5.
[47] X. Liu, X. C. Kuang, X. Hao, C. Pang, P. Xu, H. Li, Y. Liu, C. Yu, Y. Xu, D. Nan, W. Shen, Y. Fang, L. He, X. Liu, Q. Yang, *Phys. Rev. Lett.* **2017**, *118*, 076101.
[48] J. Park, H. Zheng, Y.-W. Jun, A. P. Alivisatos, *J. Am. Chem. Soc.* **2009**, *131*, 13943.
[49] J. M. Pietryga, D. J. Werder, D. J. Williams, J. L. Casson, R. D. Schaller, V. I. Klimov, J. A. Hollingsworth, *J. Am. Chem. Soc.* **2008**, *130*, 4879.
[50] M. T. Bjork, B. J. Ohlsson, T. Sass, A. I. Persson, C. Thelander, M. H. Magnusson, K. Deppert, L. R. Wallenberg, L. Samuelson, *Nano Lett.* **2002**, *2*, 87.
[51] A. Pan, H. Yang, R. Liu, R. Yu, B. Zou, Z. Wang, *J. Am. Chem. Soc.* **2005**, *127*, 15692.
[52] A. Pan, X. Wang, P. He, Q. Zhang, Q. Wan, M. Zacharias, X. Zhu, B. Zou, *Nano Lett.* **2007**, *7*, 2970.
[53] J. Xu, X. Zhuang, P. Guo, Q. Zhang, W. Huang, Q. Wan, W. Hu, X. Wang, X. Zhu, C. Fan, Z. Yang, L. Tong, X. Duan, A. Pan, *Nano Lett.* **2012**, *12*, 5003.
[54] J. Dai, P. Zhou, J. Lu, H. Zheng, J. Guo, F. Wang, N. Gu, C. Xu, *Nanoscale* **2016**, *8*, 804.

© 2019 WILEY-VCH Verlag GmbH & Co. KGaA, Weinheim

[55] X. Zhuang, P. Guo, Q. Zhang, H. Liu, D. Li, W. Hu, X. Zhu, H. Zhou, A. Pan, *Nano Res.* **2016**, *9*, 933.
[56] O. Vybornyi, S. Yakunina, M. V. Kovalenko, *Nanoscale* **2016**, *8*, 6278.
[57] G. Nedelcu, L. Protesescu, S. Yakunin, M. I. Bodnarchuk, M. J. Grotevent, M. V. Kovalenko, *Nano Lett.* **2015**, *15*, 5635.
[58] J. Y. Woo, Y. Kim, J. Bae, T. G. Kim, J. W. Kim, D. C. Lee, S. Jeong, *Chem. Mater.* **2017**, *29*, 7088.
[59] Y. Wang, X. Li, J. Song, L. Xiao, H. Zeng, H. Sun, *Adv. Mater.* **2015**, *27*, 7101.
[60] G. Li, H. Wang, T. Zhang, L. Mi, Y. Zhang, Z. Zhang, W. Zhang, Y. Jiang, *Adv. Funct. Mater.* **2016**, *26*, 8478.
[61] X. Li, Y. Wu, S. Zhang, B. Cai, Y. Gu, J. Song, H. Zeng, *Adv. Funct. Mater.* **2016**, *26*, 2435.
[62] I. Levchuk, A. Osvet, X. Tang, M. Brandl, J. D. Perea, F. Hoegl, G. J. Matt, R. Hock, M. Batentschuk, C. J. Brabec, *Nano Lett.* **2017**, *17*, 2765.
[63] M. Imran, V. Caligiuri, M. Wang, L. Goldoni, M. Prato, R. Krahne, L. De Trizio, L. Manna, *J. Am. Chem. Soc.* **2018**, *140*, 2656.
[64] K. F. Mak, C. Lee, J. Hone, J. Shan, T. F. Heinz, *Phys. Rev. Lett.* **2010**, *105*, 136805.
[65] A. Splendiani, L. Sun, Y. Zhang, T. Li, J. Kim, C. Y. Chim, G. Galli, F. Wang, *Nano Lett.* **2010**, *10*, 1271.
[66] G. Eda, H. Yamaguchi, D. Voiry, T. Fujita, M. Chen, M. Chhowalla, *Nano Lett.* **2011**, *11*, 5111.
[67] H. R. Gutierrez, N. Perea-Lopez, A. L. Elias, A. Berkdemir, B. Wang, R. Lv, F. Lopez-Urias, V. H. Crespi, H. Terrones, M. Terrones, *Nano Lett.* **2013**, *13*, 3447.
[68] J. Kang, S. Tongay, J. Zhou, J. Li, J. Wu, *Appl. Phys. Lett.* **2013**, *102*, 012111.
[69] S. Najmaei, Z. Liu, W. Zhou, X. Zou, G. Shi, S. Lei, B. I. Yakobson, J. C. Idrobo, P. M. Ajayan, J. Lou, *Nat. Mater.* **2013**, *12*, 754.
[70] A. M. van der Zande, P. Y. Huang, D. A. Chenet, T. C. Berkelbach, Y. You, G. H. Lee, T. F. Heinz, D. R. Reichman, D. A. Muller, J. C. Hone, *Nat. Mater.* **2013**, *12*, 554.
[71] X. Duan, C. Wang, J. C. Shaw, R. Cheng, Y. Chen, H. Li, X. Wu, Y. Tang, Q. Zhang, A. Pan, J. Jiang, R. Yu, Y. Huang, X. Duan, *Nat. Nanotechnol.* **2014**, *9*, 1024.
[72] Y. Gong, J. Lin, X. Wang, G. Shi, S. Lei, Z. Lin, X. Zou, G. Ye, R. Vajtai, B. I. Yakobson, H. Terrones, M. Terrones, B. K. Tay, J. Lou, S. T. Pantelides, Z. Liu, W. Zhou, P. M. Ajayan, *Nat. Mater.* **2014**, *13*, 1135.
[73] Y. Liu, J. A. Zapien, Y. Y. Shan, C.-Y. Geng, C. S. Lee, S.-T. Lee, *Adv. Mater.* **2005**, *17*, 1372.
[74] T. Kuykendall, P. Ulrich, S. Aloni, P. Yang, *Nat. Mater.* **2007**, *6*, 951.
[75] A. Pan, W. Zhou, E. S. P. Leong, R. Liu, A. H. Chin, B. Zou, C. Z. Ning, *Nano Lett.* **2009**, *9*, 784.
[76] A. Pan, R. Liu, M. Sun, C.-Z. Ning, *ACS Nano* **2010**, *4*, 671.
[77] S. Assali, I. Zardo, S. Plissard, D. Kriegner, M. A. Verheijen, G. Bauer, A. Meijerink, A. Belabbes, F. Bechstedt, J. E. Haverkort, E. P. Bakkers, *Nano Lett.* **2013**, *13*, 1559.
[78] Q. Wang, A. T. Connie, H. P. Nguyen, M. G. Kibria, S. Zhao, S. Sharif, I. Shih, Z. Mi, *Nanotechnology* **2013**, *24*, 345201.
[79] P. L. Nichols, Z. Liu, L. Yin, S. Turkdogan, F. Fan, C. Z. Ning, *Nano Lett.* **2015**, *15*, 909.
[80] X. Yuan, P. Caroff, J. Wong-Leung, H. H. Tan, C. Jagadish, *Nanoscale* **2015**, *7*, 4995.
[81] A. Berg, P. Caroff, N. Shahid, M. N. Lockrey, X. Yuan, M. T. Borgström, H. H. Tan, C. Jagadish, *Nano Res.* **2017**, *10*, 672.
[82] G. Xing, N. Mathews, S. S. Lim, N. Yantara, X. Liu, D. Sabba, M. Gratzel, S. Mhaisalkar, T. C. Sum, *Nat. Mater.* **2014**, *13*, 476.
[83] G. E. Eperon, S. D. Stranks, C. Menelaou, M. B. Johnston, L. M. Herz, H. J. Snaith, *Energy Environ. Sci.* **2014**, *7*, 982.
[84] L. Protesescu, S. Yakunin, M. I. Bodnarchuk, F. Krieg, R. Caputo, C. H. Hendon, R. X. Yang, A. Walsh, M. V. Kovalenko, *Nano Lett.* **2015**, *15*, 3692.
[85] T. C. Jellicoe, J. M. Richter, H. F. Glass, M. Tabachnyk, R. Brady, S. E. Dutton, A. Rao, R. H. Friend, D. Credgington, N. C. Greenham, M. L. Bohm, *J. Am. Chem. Soc.* **2016**, *138*, 2941.
[86] W. van der Stam, J. J. Geuchies, T. Altantzis, K. H. van den Bos, J. D. Meeldijk, S. Van Aert, S. Bals, D. Vanmaekelbergh, C. de Mello Donega, *J. Am. Chem. Soc.* **2017**, *139*, 4087.
[87] Q. Feng, Y. Zhu, J. Hong, M. Zhang, W. Duan, N. Mao, J. Wu, H. Xu, F. Dong, F. Lin, C. Jin, C. Wang, J. Zhang, L. Xie, *Adv. Mater.* **2014**, *26*, 2648.
[88] Q. Feng, N. Mao, J. Wu, H. Xu, C. Wang, J. Zhang, L. Xie, *ACS Nano* **2015**, *9*, 7450.
[89] M. Zhang, J. Wu, Y. Zhu, D. O. Dumcenco, S. Deng, Y. Chen, Y. Yang, C. Jin, S. H. Chaki, Y.-S. Huang, J. Zhang, L. Xie, *ACS Nano* **2014**, *8*, 7130.
[90] Q. Fu, L. Yang, W. Wang, A. Han, J. Huang, P. Du, Z. Fan, J. Zhang, B. Xiang, *Adv. Mater.* **2015**, *27*, 4732.
[91] Y. Huang, X. Chen, D. Zhou, H. Liu, C. Wang, J. Du, L. Ning, S. Wang, *J. Phys. Chem. C* **2016**, *120*, 5839.
[92] A. F. Rigosi, H. M. Hill, K. T. Rim, G. W. Flynn, T. F. Heinz, *Phys. Rev. B* **2016**, *94*, 075440.
[93] T. A. Shifa, F. Wang, K. Liu, K. Xu, Z. Wang, X. Zhan, C. Jiang, J. He, *Small* **2016**, *12*, 3802.
[94] P. Yu, J. Lin, L. Sun, Q. L. Le, X. Yu, G. Gao, C. H. Hsu, D. Wu, T. R. Chang, Q. Zeng, F. Liu, Q. J. Wang, H. T. Jeng, H. Lin, A. Trampert, Z. Shen, K. Suenaga, Z. Liu, *Adv. Mater.* **2017**, *29*, 1603991.
[95] O. B. Aslan, I. M. Datye, M. J. Mleczko, K. Sze Cheung, S. Krylyuk, A. Bruma, I. Kalish, A. V. Davydov, E. Pop, T. F. Heinz, *Nano Lett.* **2018**, *18*, 2485.
[96] Y. Xiao, C. Meng, X. Wu, L. Tong, *Appl. Phys. Lett.* **2011**, *99*, 023109.
[97] H. Xu, J. B. Wright, T.-S. Luk, J. J. Figiel, K. Cross, L. F. Lester, G. Balakrishnan, G. T. Wang, I. Brener, Q. Li, *Appl. Phys. Lett.* **2012**, *101*, 113106.
[98] H. Gao, A. Fu, S. C. Andrews, P. Yang, *Proc. Natl. Acad. Sci. USA* **2013**, *110*, 865.
[99] P. Xu, S. Liu, M. Tang, X. Xu, X. Lin, Z. Wu, M. ZhuGe, Z. Ren, Z. Wang, X. Liu, Z. Yang, N. Raghavan, Q. Yang, *Appl. Phys. Lett.* **2017**, *110*, 201112.
[100] A. Yang, T. B. Hoang, M. Dridi, C. Deeb, M. H. Mikkelsen, G. C. Schatz, T. W. Odom, *Nat. Commun.* **2015**, *6*, 6939.
[101] J. Li, C. Meng, Y. Liu, X. Wu, Y. Lu, Y. Ye, L. Dai, L. Tong, X. Liu, Q. Yang, *Adv. Mater.* **2013**, *25*, 833.
[102] Z. Yang, D. Wang, C. Meng, Z. Wu, Y. Wang, Y. Ma, L. Dai, X. Liu, T. Hasan, X. Liu, Q. Yang, *Nano Lett.* **2014**, *14*, 3153.
[103] X. Jiang, Q. Yang, G. Vienne, Y. Li, L. Tong, *Appl. Phys. Lett.* **2006**, *89*, 143513.
[104] S. Wu, S. Buckley, J. R. Schaibley, L. Feng, J. Yan, D. G. Mandrus, F. Hatami, W. Yao, J. Vuckovic, A. Majumdar, X. Xu, *Nature* **2015**, *520*, 69.
[105] D. Wang, M. R. Bourgeois, W. K. Lee, R. Li, D. Trivedi, M. P. Knudson, W. Wang, G. C. Schatz, T. W. Odom, *Nano Lett.* **2018**, *18*, 4549.
[106] Q. C. Sun, L. Yadgarov, R. Rosentsveig, G. Seifert, R. Tenne, *ACS Nano* **2013**, *7*, 3506.
[107] F. Urbach, *Phys. Rev.* **1953**, *92*, 1324.
[108] S. John, C. Soukoulis, M. H. Cohen, E. N. Economou, *Phys. Rev. Lett.* **1986**, *57*, 1777.
[109] A. Pan, D. Liu, R. Liu, F. Wang, X. Zhu, B. Zou, *Small* **2005**, *1*, 980.
[110] P. Lautenschlager, M. Garriga, S. Logothetidis, M. Cardona, *Phys. Rev. B* **1987**, *35*, 9174.
[111] S.-H. Wei, A. Zunger, *Phys. Rev. B* **1999**, *60*, 5404.
[112] X. Han, L. Kou, X. Lang, J. Xia, N. Wang, R. Qin, J. Lu, J. Xu, Z. Liao, X. Zhang, X. Shan, X. Song, J. Gao, W. Guo, D. Yu, *Adv. Mater.* **2009**, *21*, 4937.
[113] B. Wei, K. Zheng, Y. Ji, Y. Zhang, Z. Zhang, X. Han, *Nano Lett.* **2012**, *12*, 4595.

© 2019 WILEY-VCH Verlag GmbH & Co. KGaA, Weinheim

[114] X. Fu, Z.-M. Liao, R. Liu, F. Lin, J. Xu, R. Zhu, W. Zhong, Y. Liu, W. Guo, D. Yu, *ACS Nano* **2015**, *9*, 11960.
[115] X. Duan, Y. Huang, Y. Cui, J. Wang, C. M. Lieber, *Nature* **2001**, *409*, 66.
[116] Y. Huang, X. Duan, Y. Cui, L. J. Lauhon, K.-H. Kim, C. M. Lieber, *Science* **2001**, *294*, 1313.
[117] C.-Z. Ning, L. Dou, P. Yang, *Nat. Rev. Mater.* **2017**, *2*, 17070.
[118] F. Glas, *Phys. Rev. B* **2016**, *74*, 121302.
[119] X. Zhuang, C. Z. Ning, A. Pan, *Adv. Mater.* **2012**, *24*, 13.
[120] A. Pan, R. Liu, M. Sun, C. Z. Ning, *J. Am. Chem. Soc.* **2009**, *131*, 9502.
[121] F. Gu, Z. Yang, H. Yu, J. Xu, P. Wang, L. Tong, A. Pan, *J. Am. Chem. Soc.* **2011**, *133*, 2037.
[122] S. Turkdogan, F. Fan, C.-Z. Ning, *Adv. Funct. Mater.* **2016**, *26*, 8521.
[123] Z. Yang, J. Xu, P. Wang, X. Zhuang, A. Pan, L. Tong, *Nano Lett.* **2011**, *11*, 5085.
[124] Y. Lu, F. Gu, C. Meng, H. Yu, Y. Ma, W. Fang, L. Tong, *Opt. Express* **2013**, *21*, 22314.
[125] F. Fan, Z. Liu, L. Yin, P. L. Nichols, H. Ning, S. Turkdogan, C. Z. Ning, *Semicond. Sci. Technol.* **2013**, *28*, 065005.
[126] S. Liu, C. Li, J. J. Figiel, S. R. Brueck, I. Brener, G. T. Wang, *Nanoscale* **2015**, *7*, 9581.
[127] Z. Liu, L. Yin, H. Ning, Z. Yang, L. Tong, C.-Z. Ning, *Nano Lett.* **2013**, *13*, 4945.
[128] F. Qian, Y. Li, S. Gradecak, H. G. Park, Y. Dong, Y. Ding, Z. L. Wang, C. M. Lieber, *Nat. Mater.* **2008**, *7*, 701.
[129] M. T. Hill, Y.-S. Oei, B. Smalbrugge, Y. Zhu, T. de Vries, P. J. van Veldhoven, F. W. M. van Otten, T. J. Eijkemans, J. P. Turkiewicz, H. de Waardt, E. J. Geluk, S.-H. Kwon, Y.-H. Lee, R. Nötzel, M. K. Smit, *Nat. Photonics* **2007**, *1*, 589.
[130] D. J. Bergman, M. I. Stockman, *Phys. Rev. Lett.* **2003**, *90*, 027402.
[131] M. A. Noginov, G. Zhu, A. M. Belgrave, R. Bakker, V. M. Shalaev, E. E. Narimanov, S. Stout, E. Herz, T. Suteewong, U. Wiesner, *Nature* **2009**, *460*, 1110.
[132] R. F. Oulton, V. J. Sorger, T. Zentgraf, R. M. Ma, C. Gladden, L. Dai, G. Bartal, X. Zhang, *Nature* **2009**, *461*, 629.
[133] E. I. Galanzha, R. Weingold, D. A. Nedosekin, M. Sarimollaoglu, J. Nolan, W. Harrington, A. S. Kuchyanov, R. G. Parkhomenko, F. Watanabe, Z. Nima, A. S. Biris, A. I. Plekhanov, M. I. Stockman, V. P. Zharov, *Nat. Commun.* **2017**, *8*, 15528.
[134] M. A. Peña, J. L. G. Fierro, *Chem. Rev.* **2001**, *101*, 1981.
[135] A. Kojima, K. Teshima, Y. Shirai, T. Miyasaka, *J. Am. Chem. Soc.* **2009**, *131*, 6050.
[136] M. M. Lee, J. Teuscher, T. Miyasaka, T. N. Murakami, H. J. Snaith, *Science* **2012**, *338*, 643.
[137] N. Yantara, S. Bhaumik, F. Yan, D. Sabba, H. A. Dewi, N. Mathews, P. P. Boix, H. V. Demir, S. Mhaisalkar, *J. Phys. Chem. Lett.* **2015**, *6*, 4360.
[138] A. B. Wong, M. Lai, S. W. Eaton, Y. Yu, E. Lin, L. Dou, A. Fu, P. Yang, *Nano Lett.* **2015**, *15*, 5519.
[139] C. Murawski, K. Leo, M. C. Gather, *Adv. Mater.* **2013**, *25*, 6801.
[140] Y. Shirasaki, G. J. Supran, M. G. Bawendi, V. Bulovic, *Nat. Photonics* **2013**, *7*, 13.
[141] O. A. Jaramillo-Quintero, R. S. Sanchez, M. Rincon, I. Mora-Sero, *J. Phys. Chem. Lett.* **2015**, *6*, 1883.
[142] Z. K. Tan, R. S. Moghaddam, M. L. Lai, P. Docampo, R. Higler, F. Deschler, M. Price, A. Sadhanala, L. M. Pazos, D. Credgington, F. Hanusch, T. Bein, H. J. Snaith, R. H. Friend, *Nat. Nanotechnol.* **2014**, *9*, 687.
[143] X. Hu, X. Zhang, L. Liang, J. Bao, S. Li, W. Yang, Y. Xie, *Adv. Funct. Mater.* **2014**, *24*, 7373.
[144] M. I. Saidaminov, V. Adinolfi, R. Comin, A. L. Abdelhady, W. Peng, I. Dursun, M. Yuan, S. Hoogland, E. H. Sargent, O. M. Bakr, *Nat. Commun.* **2015**, *6*, 8724.
[145] H. Deng, D. Dong, K. Qiao, L. Bu, B. Li, D. Yang, H. E. Wang, Y. Cheng, Z. Zhao, J. Tang, H. Song, *Nanoscale* **2015**, *7*, 4163.
[146] G. Xing, M. H. Kumar, W. K. Chong, X. Liu, Y. Cai, H. Ding, M. Asta, M. Grätzel, S. Mhaisalkar, N. Mathews, T. C. Sum, *Adv. Mater.* **2016**, *28*, 8191.
[147] G. Xing, B. Wu, X. Wu, M. Li, B. Du, Q. Wei, J. Guo, E. K. L. Yeow, T. C. Sum, W. Huang, *Nat. Commun.* **2017**, *8*, 14558.
[148] K. Wu, G. Liang, Q. Shang, Y. Ren, D. Kong, T. Lian, *J. Am. Chem. Soc.* **2015**, *137*, 12792.
[149] H. Huang, A. S. Susha, S. V. Kershaw, T. F. Hung, A. L. Rogach, *Adv. Sci.* **2015**, *2*, 1500194.
[150] F. Zhang, H. Zhong, C. Chen, X. G. Wu, X. Hu, H. Huang, J. Han, B. Zou, Y. Dong, *ACS Nano* **2015**, *9*, 4533.
[151] H. Zhu, Y. Fu, F. Meng, X. Wu, Z. Gong, Q. Ding, M. V. Gustafsson, M. T. Trinh, S. Jin, X. Y. Zhu, *Nat. Mater.* **2015**, *14*, 636.
[152] D. Zhang, S. W. Eaton, Y. Yu, L. Dou, P. Yang, *J. Am. Chem. Soc.* **2015**, *137*, 9230.
[153] L. Dou, A. B. Wong, Y. Yu, M. Lai, N. Kornienko, S. W. Eaton, A. Fu, C. G. Bischak, J. Ma, T. Ding, N. S. Ginsberg, L.-W. Wang, A. P. Alivisatos, P. Yang, *Science* **2015**, *349*, 1518.
[154] K. Leng, I. Abdelwahab, I. Verzhbitskiy, M. Telychko, L. Chu, W. Fu, X. Chi, N. Guo, Z. Chen, Z. Chen, C. Zhang, *Nat. Mater.* **2018**, *17*, 908.
[155] Q. Zhang, L. Chu, F. Zhou, W. Ji, G. Eda, *Adv. Mater.* **2018**, *30*, 1704055.
[156] Z. Yang, Y. Deng, X. Zhang, S. Wang, H. Chen, S. Yang, J. Khurgin, N. X. Fang, X. Zhang, R. Ma, *Adv. Mater.* **2018**, *30*, 1704333.
[157] S. W. Eaton, M. Lai, N. A. Gibson, A. B. Wong, L. Dou, J. Ma, L. W. Wang, S. R. Leone, P. Yang, *Proc. Natl. Acad. Sci. USA* **2016**, *113*, 1993.
[158] H. Zhou, S. Yuan, X. Wang, T. Xu, X. Wang, H. Li, W. Zheng, P. Fan, Y. Li, L. Sun, A. Pan, *ACS Nano* **2017**, *11*, 1189.
[159] B. Conings, J. Drijkoningen, N. Gauquelin, A. Babayigit, J. D'Haen, L. D'Olieslaeger, A. Ethirajan, J. Verbeeck, J. Manca, E. Mosconi, F. D. Angelis, *Adv. Energy Mater.* **2015**, *5*, 1500477.
[160] M. Saliba, J. P. Correa-Baena, M. Grätzel, A. Hagfeldt, A. Abate, *Angew. Chem., Int. Ed.* **2018**, *57*, 2554.
[161] S. Yakunin, L. Protesescu, F. Krieg, M. I. Bodnarchuk, G. Nedelcu, M. Humer, G. De Luca, M. Fiebig, W. Heiss, M. V. Kovalenko, *Nat. Commun.* **2015**, *6*, 8056.
[162] W. Du, S. Zhang, J. Shi, J. Chen, Z. Wu, Y. Mi, Z. Liu, Y. Li, X. Sui, R. Wang, X. Qiu, T. Wu, Y. Xiao, Q. Zhang, X. Liu, *ACS Photonics* **2018**, *5*, 2051.
[163] Y. Fu, H. Zhu, C. C. Stoumpos, Q. Ding, J. Wang, M. G. Kanatzidis, X. Zhu, S. Jin, *ACS Nano* **2016**, *10*, 7963.
[164] J.-W. Lee, D.-H. Kim, H.-S. Kim, S.-W. Seo, S. M. Cho, N.-G. Park, *Adv. Energy Mater.* **2015**, *5*, 1501310.
[165] W. S. Yang, B. W. Park, E. H. Jung, N. J. Jeon, Y. C. Kim, D. U. Lee, S. S. Shin, J. Seo, E. K. Kim, J. H. Noh, S. I. Seok, *Science* **2017**, *356*, 1376.
[166] Y. Fu, H. Zhu, A. W. Schrader, D. Liang, Q. Ding, P. Joshi, L. Hwang, X. Y. Zhu, S. Jin, *Nano Lett.* **2016**, *16*, 1000.
[167] I. Lignos, L. Protesescu, D. B. Emiroglu, R. Maceiczyk, S. Schneider, M. V. Kovalenko, A. J. DeMello, *Nano Lett.* **2018**, *18*, 1246.
[168] C. Guhrenz, A. Benad, C. Ziegler, D. Haubold, N. Gaponik, A. Eychmüller, *Chem. Mater.* **2016**, *28*, 9033.
[169] Y. Bekenstein, B. A. Koscher, S. W. Eaton, P. Yang, A. P. Alivisatos, *J. Am. Chem. Soc.* **2015**, *137*, 16008.
[170] J. A. Sichert, Y. Tong, N. Mutz, M. Vollmer, S. Fischer, K. Z. Milowska, R. García Cortadella, B. Nickel, C. Cardenas-Daw, J. K. Stolarczyk, A. S. Urban, *Nano Lett.* **2015**, *15*, 6521.
[171] N. Zhang, K. Wang, H. Wei, Z. Gu, W. Sun, J. Li, S. Xiao, Q. Song, *J. Phys. Chem. Lett.* **2016**, *7*, 3886.
[172] L. Doua, M. Lai, C. S. Kley, Y. Yang, C. G. Bischak, D. Zhang, S. W. Eaton, N. S. Ginsberg, P. Yang, *Proc. Natl. Acad. Sci. USA* **2017**, *114*, 7216.

© 2019 WILEY-VCH Verlag GmbH & Co. KGaA, Weinheim

[173] L. Huang, Q. Gao, L.-D. Sun, H. Dong, S. Shi, T. Cai, Q. Liao, C.-H. Yan, *Adv. Mater.* **2018**, *30*, 1800596.
[174] S. Z. Butler, S. M. Hollen, L. Cao, Y. Cui, J. A. Gupta, H. R. Gutiérrez, T. F. Heinz, S. S. Hong, J. Huang, A. F. Ismach, E. Johnston-Halperin, *ACS Nano* **2013**, *7*, 2898.
[175] W. C. Tan, L. Huang, R. J. Ng, L. Wang, D. M. N. Hasan, T. J. Duffin, K. S. Kumar, C. A. Nijhuis, C. Lee, K. W. Ang, *Adv. Mater.* **2018**, *30*, 1705039.
[176] Y. Deng, Z. Luo, N. J. Conrad, H. Liu, Y. Gong, S. Najmaei, P. M. Ajayan, J. Lou, X. Xu, P. D. Ye, *ACS Nano* **2014**, *8*, 8292.
[177] Y.-Q. Bie, G. Grosso, M. Heuck, M. M. Furchi, Y. Cao, J. Zheng, D. Bunandar, E. Navarro-Moratalla, L. Zhou, D. K. Efetov, T. Taniguchi, K. Watanabe, J. Kong, D. Englund, P. Jarillo-Herrero, *Nat. Nanotechnol.* **2017**, *12*, 1124.
[178] X. Xu, W. Yao, D. Xiao, T. F. Heinz, *Nat. Phys.* **2014**, *10*, 343.
[179] K. F. Mak, J. Shan, *Nat. Photonics* **2016**, *10*, 216.
[180] S. Manzeli, D. Ovchinnikov, D. Pasquier, O. V. Yazyev, A. Kis, *Nat. Rev. Mater.* **2017**, *2*, 17033.
[181] A. Ciarrocchi, A. Avsar, D. Ovchinnikov, A. Kis, *Nat. Commun.* **2018**, *9*, 919.
[182] H. R. Gutiérrez, N. Perea-López, A. L. Elías, A. Berkdemir, B. Wang, R. Lv, F. López-Urías, V. H. Crespi, H. Terrones, M. Terrones, *Nano Lett.* **2013**, *13*, 3447.
[183] A. Autere, H. Jussila, A. Marini, J. R. M. Saavedra, Y. Dai, A. Säynätjoki, L. Karvonen, H. Yang, B. Amirsolaimani, R. A. Norwood, N. Peyghambarian, *Phys. Rev. B* **2018**, *98*, 115426.
[184] S. Najmaei, Z. Liu, W. Zhou, X. L. Zou, G. Shi, S. D. Lei, B. I. Yakobson, J. C. Idrobo, P. M. Ajayan, J. Lou, *Nat. Mater.* **2013**, *12*, 754.
[185] A. M. van der Zande, P. Y. Huang, D. A. Chenet, T. C. Berkelbach, Y. M. You, G. H. Lee, T. F. Heinz, D. R. Reichman, D. A. Muller, J. C. Hone, *Nat. Mater.* **2013**, *12*, 554.
[186] Y. Li, J. Zhang, D. Huang, H. Sun, F. Fan, J. Feng, Z. Wang, C. Z. Ning, *Nat. Nanotechnol.* **2017**, *12*, 987.
[187] Y. Ye, Z. J. Wong, X. Lu, X. Ni, H. Zhu, X. Chen, Y. Wang, X. Zhang, *Nat. Photonics* **2015**, *9*, 733.
[188] F. Lohof, A. Steinhoff, M. Florian, M. Lorke, D. Erben, F. Jahnke, C. Gies, *Nano Lett.* **2019**, *19*, 210.
[189] P. J. Pauzauskie, D. J. Sirbuly, P. Yang, *Phys. Rev. Lett.* **2006**, *96*, 143903.
[190] Z. Hu, X. Guo, L. Tong, *Appl. Phys. Lett.* **2013**, *103*, 183104.
[191] Y. Xiao, C. Meng, P. Wang, Y. Ye, H. Yu, S. Wang, F. Gu, L. Dai, L. Tong, *Nano Lett.* **2011**, *11*, 1122.
[192] R. M. Ma, X. Yin, R. F. Oulton, V. J. Sorger, X. Zhang, *Nano Lett.* **2012**, *12*, 5396.
[193] Q. Zhang, Q. Shang, J. Shi, J. Chen, R. Wang, Y. Mi, W. Du, C. Shen, R. Ma, X. Qiu, X. Liu, T. C. Sum, *ACS Photonics* **2017**, *4*, 2789.
[194] G. D. Mahan, *Phys. Rev.* **1966**, *145*, 602.
[195] D. Dunn, *Phys. Rev.* **1968**, *174*, 855.
[196] S. Kena-Cohen, S. R. Forrest, *Nat. Photonics* **2010**, *4*, 371.
[197] D. H. Li, J. Zhang, Q. Zhang, Q. H. Xiong, *Nano Lett.* **2012**, *12*, 2993.
[198] X. Liu, Q. Zhang, Q. Xiong, T. C. Sum, *Nano Lett.* **2013**, *13*, 1080.
[199] P. Guo, X. Zhuang, J. Xu, Q. Zhang, W. Hu, X. Zhu, X. Wang, Q. Wan, P. He, H. Zhou, A. Pan, *Nano Lett.* **2013**, *13*, 1251.
[200] J. Xu, X. Zhuang, P. Guo, W. Huang, W. Hu, Q. Zhang, Q. Wan, X. Zhu, Z. Yang, L. Tong, X. Duan, A. Pan, *Sci. Rep.* **2012**, *2*, 820.
[201] H. Zong, Y. Yang, C. Ma, X. Feng, T. Wei, W. Yang, J. Li, J. Li, L. You, J. Zhang, M. Li, C. Pan, X. Hu, B. Shen, *ACS Nano* **2017**, *11*, 5808.
[202] E. Burstein, *Phys. Rev.* **1954**, *93*, 632.
[203] T. S. Moss, *Proc. Phys. Soc., Sect. B* **1954**, *67*, 775.
[204] X. Liu, Q. Zhang, J. N. Yip, Q. Xiong, T. C. Sum, *Nano Lett.* **2013**, *13*, 5336.
[205] B. Mayer, D. Rudolph, J. Schnell, S. Morkotter, J. Winnerl, J. Treu, K. Muller, G. Bracher, G. Abstreiter, G. Koblmuller, J. J. Finley, *Nat. Commun.* **2013**, *4*, 2931.
[206] J. Xing, X. F. Liu, Q. Zhang, S. T. Ha, Y. W. Yuan, C. Shen, T. C. Sum, Q. Xiong, *Nano Lett.* **2015**, *15*, 4571.
[207] W. Shan, J. W. Ager, K. M. Yu, W. Walukiewicz, E. E. Haller, M. C. Martin, W. R. McKinney, W. Yang, *J. Appl. Phys.* **1999**, *85*, 8505.
[208] S. Strite, H. Morkoç, *J. Vac. Sci. Technol., B: Microelectron. Nanometer Struct. – Process., Meas., Phenom.* **1992**, *10*, 1237.
[209] Z. L. Wang, *Adv. Mater.* **2007**, *19*, 889.
[210] Z. L. Wang, *Nano Today* **2010**, *5*, 540.
[211] Q. Yang, W. H. Wang, S. Xu, Z. L. Wang, *Nano Lett.* **2011**, *11*, 4012.
[212] Q. Yang, Y. Liu, C. F. Pan, J. Chen, X. N. Wen, Z. L. Wang, *Nano Lett.* **2013**, *13*, 607.
[213] J. Lu, C. Xu, F. Li, Z. Yang, Y. Peng, X. Li, M. Que, C. Pan, Z. L. Wang, *ACS Nano* **2018**, *12*, 11899.
[214] M.-K. Kim, A. M. Lakhani, M. C. Wu, *Opt. Express* **2011**, *19*, 23504.
[215] R. S. Tucker, *IEEE J. Sel. Top. Quantum Electron.* **2011**, *17*, 261.
[216] D. A. B. Miller, *Proc. IEEE* **2009**, *97*, 1166.
[217] W. Y. Lin, C. Y. Chen, H. H. Lu, C. H. Chang, Y. P. Lin, H. C. Lin, H. W. Wu, *Opt. Express* **2012**, *20*, 9919.
[218] G. Cossu, A. M. Khalid, P. Choudhury, R. Corsini, E. Ciaramella, *Opt. Express* **2012**, *20*, B501.
[219] T. W. Hansch, I. S. Shahin, A. L. Schawlow, *Phys. Rev. Lett.* **1971**, *27*, 707.
[220] E. D. Hinkley, P. L. Kelly, *Science* **1971**, *171*, 635.
[221] X. Y. Wang, Y. L. Wang, S. Wang, B. Li, X. W. Zhang, L. Dai, M. R. Ma, *Nanophotonics* **2017**, *6*, 472.
[222] S. Wang, B. Li, X. Y. Wang, H. Z. Chen, Y. L. Wang, X. W. Zhang, L. Dai, R. M. Ma, *ACS Photonics* **2017**, *4*, 1355.
[223] S. Cho, M. Humar, N. Martino, S. H. Yun, *Phys. Rev. Lett.* **2016**, *117*, 193902.
[224] X. Liu, C. Kuang, X. Hao, C. Pang, P. Xu, H. Li, Y. Liu, C. Yu, Y. Xu, D. Nan, W. Shen, *Phys. Rev. Lett.* **2017**, *118*, 076101.

© 2019 WILEY-VCH Verlag GmbH & Co. KGaA, Weinheim